CHAPTER 1

Introduction to Photophysics and Photochemistry

Shawkat M. Aly,[1] **Charles E. Carraher Jr.,**[2] **and Pierre D. Harvey**[1]

[1]*Département de Chimie, Université de Sherbrooke, Sherbrooke, PQ, Canada J1K 2R1*

[2]*Department of Chemistry and Biochemistry, Florida Atlantic University, Boca Raton, FL 33431*

CONTENTS

I. GENERAL

Photophysics and photochemistry both deal with the impact of energy in the form of photons on materials. Photochemistry focuses on the chemistry involved as a material is impacted by photons, whereas photophysics deals with physical changes that result from the impact of photons. This chapter will focus on some of the basic principles related to photophysics and photochemistry followed by general examples. Finally, these principles will be related to photosynthesis. In many ways, there is a great similarity between a material's behavior when struck by photons, whether the material is small or macromolecular. Differences are related to size and the ability of polymers to transfer the effects of radiation from one site to another within the chain or macromolecular complex.

The importance of the interaction with photons in the natural world can hardly be overstated. It forms the basis for photosynthesis converting carbon dioxide and water into more complex plant-associated structures. This is effectively accomplished employing chlorophyll as the catalytic site (this topic will be dealt with more fully later in the chapter). Chlorophyll contains a metal atom within a polymeric matrix, so it illustrates the importance of such metal–polymer combinations. Today, with the rebirth of green materials and green chemistry use of clean fuel—namely, sunlight—is increasing in both interest and understanding.

Polymer photochemistry and physics have been recently reviewed, and readers are encouraged to investigate this further in the suggested readings given at the end of the chapter. Here, we introduce some of the basic concepts of photophysics and photochemistry. We also illustrate the use of photochemistry and photophysics in the important area of solar energy conversion.

II. PHOTOPHYSICS AND PHOTOCHEMISTRY

Photophysics involves the absorption, transfer, movement, and emission of electromagnetic, light, energy without chemical reactions. By comparison, photochemistry involves the interaction of electromagnetic energy that results in chemical reactions. Let us briefly review the two major types of spectroscopy with respect to light. In absorption, the detector is placed along the direction of the incoming light and the transmitted light is measured. In emission studies, the detector is placed at some angle, generally 90°, away from the incoming light.

When absorption of light occurs, the resulting polymer, $P*$, contains excess energy and is said to be excited.

$$P + h\nu \rightarrow P* \tag{1}$$

The light can be simply reemitted.

$$P* \rightarrow h\nu + P \tag{2}$$

Of much greater interest is light migration, either along the polymer backbone or to another chain. This migration allows the energy to move to a site of interest. Thus, for plants, the site of interest is chlorophyll. These 'light-gathering' sites are referred to as *antennas*. Natural antennas include chlorophyll, carotenoids, and special pigment-containing proteins. These antenna sites harvest the light by absorbing the light photon and storing it in the form of an electron, which is promoted to an excited singlet energy state (or other energy state) by the absorbed light.

Bimolecular occurrences can occur, leading to an electronic relaxation called *quenching*. In this approach $P*$ finds another molecule or part of the same chain, A, transferring the energy to A.

$$P* + A \rightarrow P + A* \tag{3}$$

Generally, the quenching molecule or site is initially in its ground state.

Eliminating chemical rearrangements, quenching most likely ends with electronic energy transfer, complex formation, or increased nonradioactive decay. Electronic energy transfer involves an exothermic process, in which part of the energy is absorbed as heat and part is emitted as fluorescence or phosphorescence radiation. Polarized light is taken on in fluorescence depolarization, also known as *luminescence anisotropy*. Thus if the chain segments are moving at about the same rate as the reemission, part of the light is depolarized. The extent of depolarization is then a measure of the segmental chain motions.

Complex formation is important in photophysics. Two terms need to be described here. First, an *exciplex* is an excited state complex formed between

two different kinds of molecules, one that is excited and one that is in its ground state. The second term, *excimer*, is similar, except the complex is formed between like molecules. Here we will focus on excimer complexes that form between two like polymer chains or within the same polymer chain. Such complexes can be formed between two aromatic structures. Resonance interactions between aromatic structures, such as two phenyl rings in polystyrene, give a weak intermolecular force formed from attractions between the π-electrons of the two aromatic entities. Excimers involving such aromatic structures give strong fluorescence.

Excimer formation can be described as follows where [PP]* is the excimer.

$$P* + P \rightarrow [PP]* \tag{4}$$

The excimer decays, giving two ground state aromatic sites and emission of fluorescence.

$$[PP]* \rightarrow h\nu + 2P \tag{5}$$

As always, the energy of the light emitted is less than that originally taken on. Through studying the amount and energy of the fluorescence, radiation decay rates, depolarization effects, excimer stability, and structure can be determined.

III. LIGHT ABSORPTION

Light is composed of particles known as photons, each of which has the energy of Planck's quantum, hc/λ; where h is Plank's constant, c is velocity of light, and λ is the wavelength of the radiation. Light has dualistic properties of both waves and particles; ejection of electrons from an atom as a result of light bombardment is due to the particle behavior, whereas the observed light diffraction at gratings is attributed to the wave properties. The different processes related to light interactions with molecules can be represented as in Figure 1.

The absorption of light by materials produces physical and chemical changes. On the negative side, such absorption can lead to discoloration generally as a response to unwanted changes in the material's structure. Absorption also can lead to a loss in physical properties, such as strength. In the biological world, it is responsible for a multitude of problems, including skin cancer. It is one of the chief modes of weathering by materials. Our focus here is on the positive changes effected by the absorption of light. Absorption of light has intentionally resulted in polymer cross-linking and associated insolubilization. This forms the basis for coatings and negative-lithographic resists. Light-induced chain breakage is the basis for positive-lithographic resists.
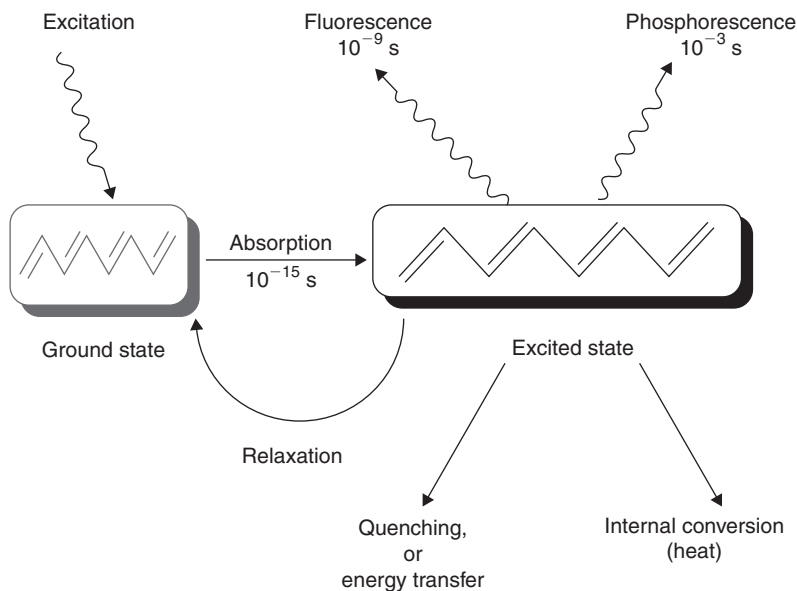
FIGURE 1. Different processes associated with light interaction with a molecule.

Photoconductivity forms the basis for photocopying, and photovoltaic effects form the basis for solar cells being developed to harvest light energy.

It is important to remember that the basic laws governing small and large molecules are the same.

The Grotthus-Draper law states that photophysical/photochemical reactions occur only when a photon of light is absorbed. This forms the basis for the First Law of Photochemistry—that is, only light that is absorbed can have a photophysical/photochemical effect.

We can write this as follows.

$$M + \text{light} \rightarrow M^* \tag{6}$$

where M^* is M after it has taken on some light energy acquired during a photochemical reaction. The asterisk is used to show that M is now in an excited state.

Optical transmittance, T, is a measure of how much light that enters a sample is absorbed.

$$T = I/I_o \tag{7}$$

If no light is absorbed then $I = I_o$. Low transmittance values indicate that lots of the light has been absorbed.

Most spectrophotometers give their results in optical absorbency, A, or optical density, which is defined as

$$A = \log(I/I_{\mathrm{o}}) \tag{8}$$

so that

$$A = \log(1/T) = -\log T \tag{9}$$

Beer's law states that A, the absorbance of chromophores, increases in proportion to the concentration of the chromophores, where k is a constant.

$$A = kc \tag{10}$$

Beer's law predicts a straight-line relationship between absorbance and concentration and is often used to determine the concentration of an unknown after construction of the known absorbance verses concentration line.

The optical path, l, is the distance the light travels through the sample. This is seen in looking at the color in a swimming pool, where the water is deeper colored at the deep end because the optical path is greater. This is expressed by Lambert's law, where k' is another empirical constant.

$$A = k'l \tag{11}$$

To the eye some colors appear similar but may differ in intensity, when c and l are the same. These solutions have a larger molar absorption coefficient, ε, meaning they adsorb more. The larger the adsorption coefficient the more the material adsorbs.

The Beer-Lambert law combines the two laws, giving

$$A = \varepsilon lc \tag{12}$$

The proportionality constant in the Lambert's law is ε.

The extinction coefficients of chromophores vary widely from <100 1/Mcm, for a so-called forbidden transition, to greater than 10^5 1/Mcm for fully allowed transitions.

We can redefine the elements of the Beer-Lambert law, where l is the sample thickness and c is the molar concentration of chromophores. This can be rearranged to determine the penetration depth of light into a polymer material. Here l is defined as the path length, where 90% of the light of a particular wavelength is absorbed so A approaches 1, giving

$$l(\text{in } \mu\text{m}) = 10^4 \varepsilon c \tag{13}$$

This relationship holds when the polymer chromophore (or any chromophore) is uniformly distributed in a solution or bulk. In polymers with a high chromophore concentration, l is small and the photochemical/photophysical phenomenon occurs largely in a thin surface area.

Let us briefly examine the color of a red wine. The wine contains color sites, or chromophores. The photons that are not captured pass through and give us the red coloration. We see color because a chromophore interacts with light.

Molecules that absorb photons of energy corresponding to wavelengths in the range 190 nm to $\sim$1000 nm absorb in the UV-VIS region of the spectrum. The molecule that absorbs a photon of light becomes excited. The energy that is absorbed can be translated into rotational, vibrational, or electronic modes. The quantized internal energy E_{int} of a molecule in its electronic ground or excited state can be approximated, with sufficient accuracy for analytical purposes, by

$$E_{int} = E_{el} + E_{vib} + E_{rot} \tag{14}$$

where E_{el}, E_{vib}, and E_{rot} are the electronic, vibrational, and rotational energies, respectively. According to the Born-Oppenheimer approximation, electronic transitions are much faster than atomic motion. Upon excitation, electronic transitions occur in about 10^{-15} s, which is very fast compared to the characteristic time scale for molecular vibrations (10^{-10} to 10^{-12} s).[1] Hence the influence of vibrational and rotational motions on electronic states should be almost negligible. Franck-Condon stated that electronic transition is most likely to occur without changes in the position of the nuclei in the molecular entity and its environment. It is then possible to describe the molecular energy by a potential energy diagram in which the vibrational energies are superimposed upon the electronic curves (Fig. 2).

For most molecules, only one or two lower energy electronic transitions are normally postulated. Thus one would expect that the UV-VIS spectrum would be relatively simple. This is often not the case. The question is, Why are many bands often exhibiting additional features? The answer lies in the Franck-Condon principle, by which vibronic couplings are possible for polyatomic molecules. Indeed, both vibronic and electronic transitions will be observed in the spectrum, generating vibrationally structured bands, and sometimes even leading to broad unresolved bands.[2] Each resolved absorption peak corresponds to a vibronic transition, which is a particular electronic transition coupled with a vibrational mode belonging to the chromophore. For solids (when possible) and liquids, the rotational lines are broad and overlapping, so that no rotational structure is distinguishable.

To apply this concept for a simple diatomic molecule, let's consider the example given in Figure 3. At room temperature, according to the Boltzman distribution, most of the molecules are in the lowest vibrational level (ν) of the ground state (i.e., $\nu = 0$). The absorption spectrum presented in Figure 3b exhibits, in addition to the pure electronic transition (the so-called 0-0
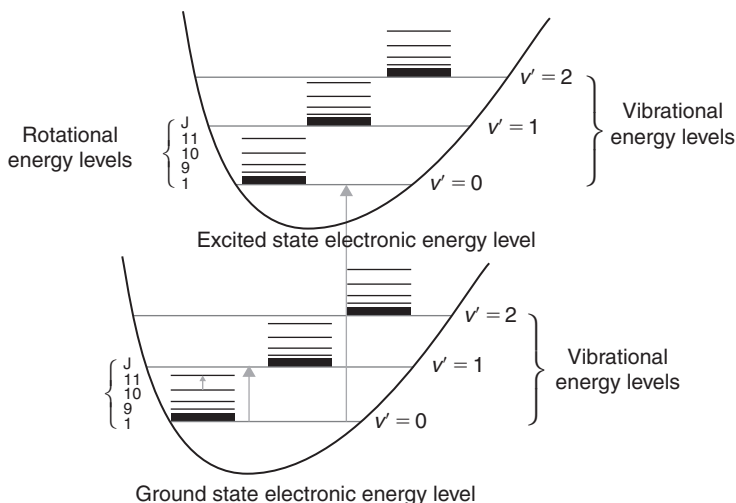
FIGURE 2. The relative ordering of electronic, vibrational, and rotational energy levels. (Modified from Ref. 1.)
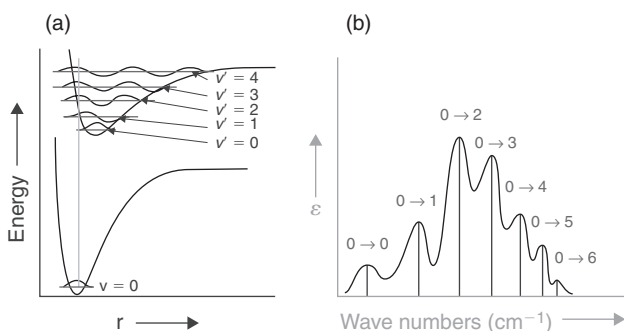

FIGURE 3. (a) Potential energy diagram for a diatomic molecule, illustrating the Franck-Condon excitation. (b) Intensity distribution among vibronic bands as determined by the Franck-Condon principle. (Modified from Ref. 2.)

transition), several vibronic peaks whose intensities depend on the relative position and shape of the potential curve.

The transition from the ground to the excited state, where the excitation goes from $\nu = 0$ (in the ground state) to $\nu = 2$ (in the excited state), is the most probable for vertical transitions because it falls on the highest point in the vibrational probability curve in the excited state. Yet many additional transitions occur, so that the fine structure of the vibronic broad band is a result of the probabilities for the different transitions between the vibronic levels.

Note that, there are two kinds of spectra—namely, excitation and absorption. The absorption and excitation spectra are distinct but usually overlap,
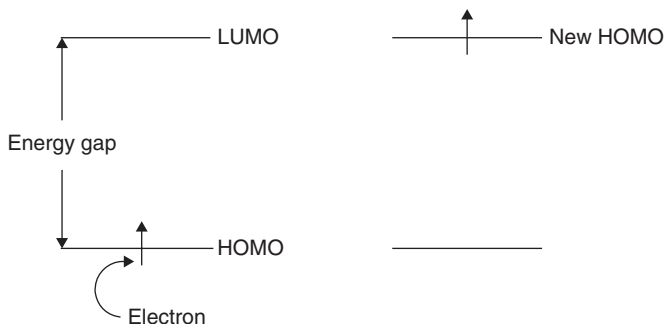
FIGURE 4. A photon being absorbed by a single molecule of chromophore.

sometimes to the extent that they are nearly indistinguishable. The excitation spectrum is the spectrum of light emitted by the material as a function of the excitation wavelength. The absorption spectrum is the spectrum of light absorbed by the material as a function of wavelength. The origin of the occasional discrepancies between the excitation and absorption spectra are due to the differences in structures between the ground and the excited states or the presence of photo reactions or the presence of nonradiative processes that relax the molecule to the ground state without passing through the luminescent states (i.e., S_1 and T_1).

Visible color is normally a result of changes in the electron states. Molecules that reside in the lowest energy level are said to be in the ground state or unexcited state. We will restrict our attention to the electrons that are in the highest occupied molecular orbital (HOMO) and the lowest unoccupied molecular orbital (LUMO). These orbitals are often referred to as the frontier orbitals.

Excitation of photons results in the movement of electrons from the HOMO to the LUMO (Fig. 4).

Photon energies can vary. Only one photon can be accepted at a time by an obtital. This is stated in the Stark-Einstein law also known as the Second Law of Photochemistry—if a species absorbs radiation, then one particle (molecule, ion, atom, etc.) is excited for each quantum of radiation (photon) that is absorbed.

Remember that a powerful lamp will have a greater photon flux than a weaker lamp. Further, photons enter a system one photon at a time. Thus every photon absorbed does not result in bond breakage or other possible measurable effect. The quantum yield, ϕ, is a measure of the effectiveness for effecting the desired outcome, possibly bond breakage and formation of free radicals.

$$\phi = \text{number of molecules of reactant consumed}/ \\ \text{number of photons consumed} \tag{15}$$

Quantum yields can provide information about the electronic excited state relaxation processes, such as the rates of radiative and nonradiative

processes. Moreover, they can also find applications in the determination of chemical structures and sample purity.[3] The emission quantum yield can be defined as the fraction of molecules that emits a photon after direct excitation by a light source.[4] So emission quantum yield is also a measure of the relative probability for radiative relaxation of the electronically excited molecules.

Quantum yields vary greatly; the photons range from very ineffective (10^{-6}) to very effective (10^6). Values >1 indicate that some chain reaction, such as in a polymerization, occurred.

We often differentiate between the primary quantum yield, which focuses on only the first event (here the quantum yield cannot be >1), and secondary quantum yield, which focuses on the total number of molecules formed via secondary reactions (here the quantum yield can be high). The common emission quantum yield measurement involves the comparison of a very dilute solution of the studied sample with a solution of approximately equal optical density of a compound of known quantum yield (standard reference). The quantum yield of an unknown sample is related to that of a standard by equation 16.[5]

$$\Phi_u = \left[\frac{(A_s F_u n^2)}{(A_u F_s n_0^2)} \right] \Phi_s \tag{16}$$

where, the subscript u refers to 'unknown', and s to the comparative standard; Φ is the quantum yield, A is the absorbance at a given excitation wavelength, F is the integrated emission area across the band, and n and n_0 are the refractive indices of the solvent containing the unknown and the standard, respectively.

For the most accurate measurements, both the sample and standard solutions should have low absorptions (≤ 0.05) and have the similar absorptions at the same excitation wavelength.[5]

IV. LUMINESCENCE

Luminescence is a form of cold body radiation. Older TV screens operated on the principle of luminescence, by which the emission of light occurs when they are relatively cool. Luminescence includes phosphorescence and fluorescence. In a TV, electrons are accelerated by a large electron gun sitting behind the screen. In the black-and-white sets, the electrons slam into the screen surface, which is coated with a phosphor that emits light when hit with an electron. Only the phosphor that is hit with these electrons gives off light. The same principle operates in the old-generation color TVs, except the inside of the screen is coated with thousands of groups of dots, each group consisting of three dots (red, green, and blue). The kinetic energy of the electrons is absorbed by the phosphor and reemitted as visible light to be seen by us.

Fluorescence involves the molecular absorption of a photon that triggers the emission of a photon of longer wavelength (less energy; Fig. 2). The energy difference ends up as rotational, vibrational, or heat energy loses.

Here excitation is described as

$$S_{\mathrm{o}} + h\nu_{\mathrm{ex}} \rightarrow S_1 \tag{17}$$

and emission as

$$S_1 \rightarrow h\nu_{\mathrm{em}} + S_{\mathrm{o}} \tag{18}$$

where S_{o} is the ground state and S_1 is the first excited state.

The excited state molecule can relax by a number of different, generally competing pathways. One of these pathways is conversion to a triplet state that can subsequently relax through phosphorescence or some secondary nonradiative step. Relaxation of the excited state can also occur through fluorescence quenching. Molecular oxygen is a particularly efficient quenching molecule because of its unusual triplet ground state.

Watch hands that can be seen in the dark allow us to read the time without turning on a light. These watch hands typically are painted with phosphorescent paint. Like fluorescence, phosphorescence is the emission of light by a material previously hit by electromagnetic radiation. Unlike fluorescence, phosphorescence emission persists as an afterglow for some time after the radiation has stopped. The shorter end of the duration for continued light emission is 10^{-3} s but the process can persist for hours or days.

An energy level diagram representing the different states and transitions is called a Jablonski diagram or a state diagram. The Jablonski diagram was first introduced in 1935; a slightly modified version is presented in Figure 5.[2,6] The different energy levels are given in this figure, where S_0 represents the electronic ground state and S_1 and S_2 represent the first and second singlet excited states, respectively. The first and second triplet states are denoted T_1 and T_2, respectively.

In the singlet states, all electron spins are paired and the multiplicity of this state is 1. The subscript indicates the relative energetic position (electronic level) compared to other states of the same multiplicity. On the other hand, in the triplet states, two electrons are no longer antiparallel and the multiplicity is 3. The triplet state is more stable than the singlet counterpart (S) and the source for this energy difference is created by the difference in the Coulomb repulsion energies between the two electrons in the singlet versus triplet states and the increase in degree of freedom of the magnetic spins. Because the electrons in the singlet excited state are confined within the same orbital, the Coulomb repulsive energy between them is higher than in the triplet excited state where these electrons are now in separate orbitals. The splitting between these two states (S-T) also depends on the nature of the orbital.
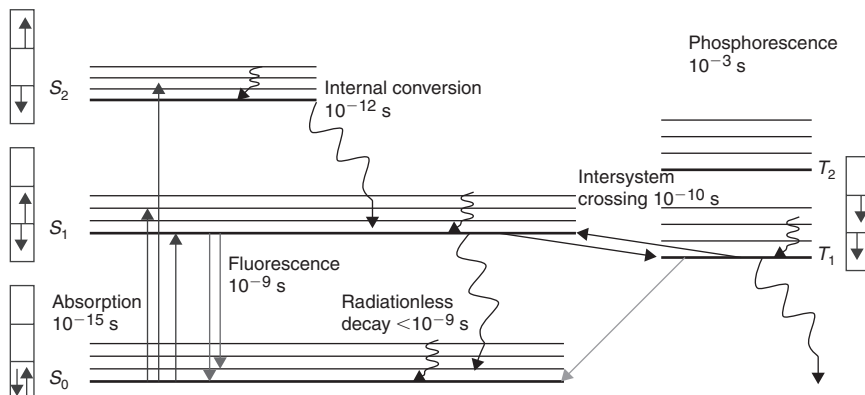
FIGURE 5. Jablonski diagram showing the various processes associated with light absorption and their time scale. *Arrows in boxes*, the relative spin states of the paired electrons. (Modified from Ref. 2.)

Let's consider a case where the two orbitals involved in a transition are similar (i.e., two p-orbitals of an atom, or two π-orbitals of an aromatic hydrocarbon). For this situation the overlap between them may be high, and the two electrons will be forced to be close to each other resulting in the S-T splitting being large. The other situation is the case where the two orbitals are different (i.e., $n \rightarrow \pi^*$ or $d \rightarrow \pi$ transitions), resulting in a small overlap. Because the overlap is small, the two electrons will have their own region of space in which to spread, resulting in a minimization of the repulsive interactions between them, and hence the S-T splitting will be small.

Absorption occurs on a time scale of about 10^{-15} s.[2] When inducing the promotion of an electron from the HOMO to the LUMO, the molecule passes from an electronic ground singlet state S_0 (for diamagnetic molecules) to a vibrational level of an upper singlet or triplet excited state S_n or T_n, respectively. The energy of the absorbed photon determines which excited state is accessible. After a while, the excited molecule relaxes to the ground state via either radiative (with emission of light) or nonradiative (without emission of light) processes. The radiative processes (for diamagnetic molecules) include either the spin-allowed fluorescence or spin-forbidden phosphorescence. Nonradiative processes include intersystem crossings (ISCs), a process allowing a molecule to relax from the S_n to the T_n manifolds, and internal conversions (IC and IP), a stepwise (vibrational) energy loss process relaxing molecules from upper excited states to any other state without or with a change in state multiplicity, respectively.[2]

An internal conversion (IC) is observed when a molecule lying in the excited state relaxes to a lower excited state. This is a radiationless transition between two different electronic states of the same multiplicity and is possible when there is a good overlap of the vibrational wave functions (or probabilities) that are involved between the two states (beginning and final).
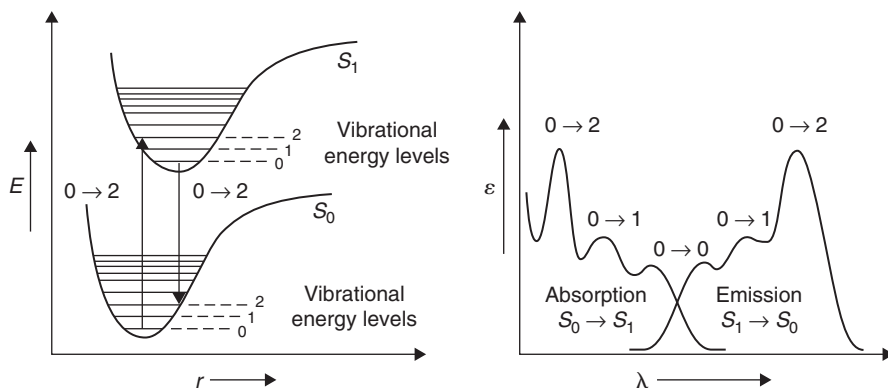
FIGURE 6. Potential energy curves and vibronic structure in fluorescence spectra. (Modified from Ref. 2.)

Internal conversion occurs on a time scale of 10^{-12} s, which is a time scale associated with molecular vibrations. A similar process occurs for an internal conversion, (IP) when it is accompanied by a change in multiplicity (such as triplet T_1 down to S_0). Upon nonradiative relaxation, heat is released. This heat is transferred to the media by collision with neighboring molecules.

Fluorescence (Fig. 6) is a radiative process in a diamagnetic molecule involving two states (excited and ground states) of the same multiplicity (e.g., $S_1 \rightarrow S_0$ and $S_2 \rightarrow S_0$). Fluorescence spectra show the intensity of the emitted light versus the wavelength. A fluorescence spectrum is obtained by initial irradiation of the sample, normally at a single wavelength, where the molecule absorbs light. The lifetime of fluorescence is typically on the order of $10^{-8} - 10^{-9}$ s (i.e., an ns time scale) for organic molecules and faster for metal-containing compounds (10^{-10} s or shorter).

In general, the fluorescence band, typically $S_1 \rightarrow S_0$, is a mirror image of the absorption band ($S_0 \rightarrow S_1$), as illustrated in Figures 6 and 7. This is particularly true for rigid molecules, such as aromatics. Once again, the Franck-Condon principle is applicable, and hence the presence of vibronic bands is expected in the fluorescence band. However there are numerous exceptions to this rule, particularly when the molecule changes geometry in its excited state. Another observation is that the emission is usually red shifted in comparison with absorption. This is because the vibronic energy levels involved are lower for fluorescence and higher for absorption, as illustrated in Figure 6. The difference in wavelength between the 0-0 absorption and the emission band is usually known as the *Stokes shift*. The magnitude of the Stokes shift gives an indication of the extent of geometry difference between the ground and excited states of a molecule as well as the solvent−solute reorganization.[2]

Another nonradiative process that can take place is known as *intersystem crossing* from a singlet to a triplet or triplet to a singlet state. This process is very rapid for metal-containing compounds. This process can take place on a

time scale of $\sim 10^{-6}-10^{-8}$ s for an organic molecule, while for organometallics it is $\sim 10^{-11}$ s. This rate enhancement is due to spin-orbit coupling present in the metal-containing systems—that is, an interaction between the spin angular momentum and the orbital angular momentum, which allows mixing of the spin angular momentum with the orbital angular momentum of S_n and T_n states. Thus these singlet and triplet states are no longer "pure" singlets and triplets, and the transition from one state to the other is less forbidden by multiplicity rules. A rate increase in intersystem crossing can also be achieved by the heavy atom effect,[7] arising from an increased mixing of spin and orbital quantum number with increased atomic number. This is accomplished either through the introduction of heavy atoms into the molecule via chemical bonding (internal heavy atom effect) or with the solvent (external heavy atom effect). The spin-orbit interaction energy of atoms grows with the fourth power of the atomic number Z.

In addition to the increase in the intersystem crossing rate, heavy atoms exert more effects, which can be summarized as follows. Their presence acts (1) to decrease the phosphorescence lifetime due to an increase in the non-radiative rates, (2) to decrease the fluorescence lifetime, and (3) to increase the phosphorescence quantum yield. The presence of a heavy atom affects not only the rate for intersystem crossing but also the energy gap between the singlet and the triplet states, where the rate for the intersystem crossing increases as the energy gap between S_1 and T_1 decreases. Moreover, the nature of the excited state exerts an important effect on the intersystem crossing. For example the $S_1(n,\pi^*) \rightarrow T_2(\pi,\pi^*)$ (e.g., as in benzophenone) transition occurs almost three orders of magnitude faster than the $S_1(\pi,\pi^*) \rightarrow T_2(\pi,\pi^*)$ transition (e.g., as in anthracene)[6].
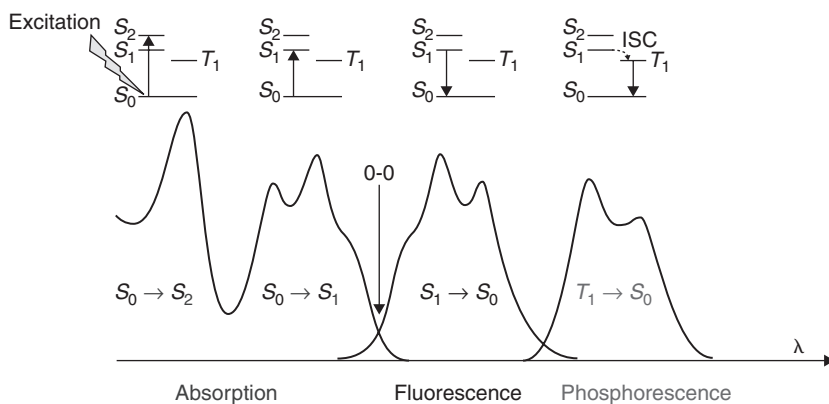

FIGURE 7. Relative positions of absorption, fluorescence, and phosphorescence The 0-0 peak is common to both absorption and fluorescence spectra (see Fig. 6). *ISC*, Intersystem crossing. (Modified from Ref. 2.)

Relaxation of triplet state molecules to the ground state can be achieved by either internal conversion (nonradiative IP) or phosphorescence (radiative). Emissions from triplet states (i.e., phosphorescence) exhibit longer lifetimes than fluorescence. These long-lived emissions occur on time scale of 10^{-3} s for organic samples and $10^{-5}-10^{-7}$ s for metal-containing species. This difference between the fluorescence and the phosphorescence is associated with the fact that it involves a spin-forbidden electronic transition. Moreover, as already noted, the phosphorescence bands are always red shifted in comparison with their fluorescence counterpart because of the relative stability of the triplet state compared to the singlet manifold (Fig. 7).[2] Nonradiative processes in the triplet states increase exponentially with a decrease in triplet energies (energy gap law). Hence phosphorescence is more difficult to observe when the triplet states are present in very low energy levels. It is also often easier to observe phosphorescence at lower temperatures, at which the thermal decay is further inhibited.[8]

V. EMISSION LIFETIME

The luminescence lifetime is the average time the molecule remains in its excited state before the photon is emitted. From a kinetic viewpoint, the lifetime can be defined by the rate of depopulation of the excited (singlet or triplet) states following an optical excitation from the ground state.[9] Luminescence generally follows first-order kinetics and can be described as follows.

$$[S_1] = [S_1]_o e^{-\Gamma t} \tag{19}$$

where $[S_1]$ is the concentration of the excited state molecules at time t, $[S_1]_o$ is the initial concentration and Γ is the decay rate or inverse of the luminescence lifetime.
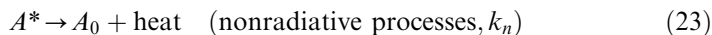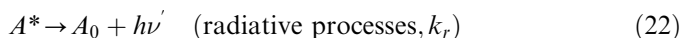
Various radative and nonradiative processes can decrease the excited state population. Here, the overall or total decay rate is the sum of these rates:

$$\Gamma_{\text{total}} = \Gamma_{\text{radiative}} + \Gamma_{\text{nonradiative}} \tag{20}$$

For a complete photophysical study, it is essential to study not only the emission spectrum but also the time domain because it can reveal a great deal of information about the rates and hence the kinetics of intramolecular and intermolecular processes. The fundamental techniques used to characterize emission lifetimes of the fluorescence and the phosphorescence are briefly described next.

When a molecule is excited (eq. 21), it is promoted from the ground to the excited state. This excited molecule can then relax to the ground state after

loosing its extra energy gained from the exciting source via a radiative (eq. 22) and nonradiative (eq. 23) processes:

$$A_0 + h\nu \rightarrow A^* \tag{21}$$

$$A^* \rightarrow A_0 + h\nu' \quad \text{(radiative processes, } k_r) \tag{22}$$

$$A^* \rightarrow A_0 + \text{heat} \quad \text{(nonradiative processes, } k_n) \tag{23}$$

Therefore, we can write

$$-\frac{d[A^*]}{dt} = (k_r + k_n)[A^*]t = -\frac{t}{\tau} \tag{24}$$

where $[A^*]$ is the concentration of the species A in its excited state at a given time t and k_r and k_n are the rate constants for the radiative and nonradiative processes, respectively.

The relative concentration of A^* is given by

$$\ln \frac{[A^*]_t}{[A^*]_{t=0}} = -(k_r + k_n)t = -\frac{t}{\tau} \tag{25}$$

Hence the mean lifetime (τ) of $[A^*]$ is

$$\tau = 1/(k_r + k_n) \tag{26}$$

where k_r and k_n are the rate constants for the radiative and nonradiative processes, respectively, represented by equations 22 and 23.

Thus the measured unimolecular radiative lifetime is the reciprocal of the sum of the unimolecular rate constants for all the deactivation processes. The general form of the equation is given by

$$\tau = \frac{1}{\sum_i k_i} \tag{27}$$

where τ is observed radiative lifetime and the rate constant k_i represents the unimolecular or pseudo-unimolecular processes that deactivate A^*.[10]

The lifetime can be measured from a time-resolved experiment in which a very short pulse excitation is made, followed by measurement of the time-dependent intensity, as illustrated in Figure 8.

The intensity decays are often measured through a polarizer oriented at some angle such as about 55° from the vertical z-axis to avoid the effects of
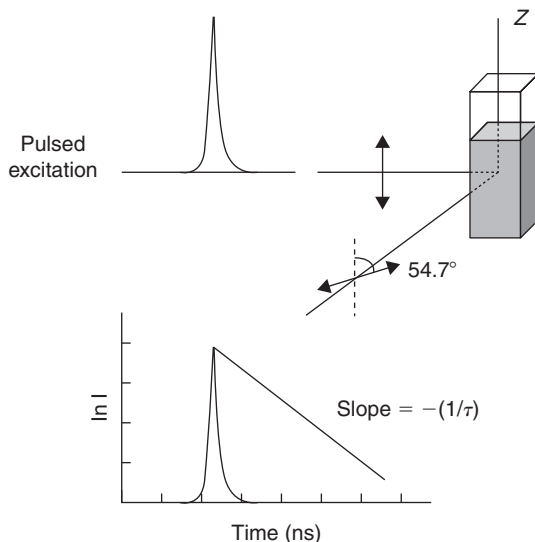
FIGURE 8. Time-domain lifetime measurement. (Modified from Ref. 11.)

anisotropy on the intensity decay.[11] Then the log of the recorded intensity is plotted against time to obtain a straight line predictable from the integration of the equation 24. The slope of this line is the negative reciprocal of the lifetime. When more than one lifetime is present in the decay traces, then there is more than one radiative pathway to relaxation. This often signifies that more than one species is emitting light at the excitation wavelength. The analysis of such multicomponent decays involves the deconvolution of an equation of the same form of equation 24 where a weighing factor for each component is added to each component.

One possible explanation for the polyexponential curves can be an exciton process. The exciton phenomenon is a delocalization of excitation energy through a material. A description of this is given in Figure 9. It shows a one-dimensional coordination or organometallic polymer denoted by $-|M_n|\text{-}|M_n|$ $\text{-}|M_n|\text{-}|M_n|\text{-}$, where M_n represent a mononuclear ($n = 1$) or polynuclear center ($n > 1$). The incident irradiation is absorbed by a single chromophore, $|M_n|$, along the backbone, and then this stored energy is reversibly transmitted via an energy transfer process to the neighboring chromophore (with no thermodynamic gain or loss; i.e., $\Delta G^0 = 0$). This newly created chromophore can reemit, or not, the light ($h\nu_2$, $h\nu_3$, $h\nu_4$,...) at a given moment.

The interactions between the different units in the excited states are called *excimers*. These excimers can be excited dimers, trimers, tetramers, etc. These excited oligomers have different wavelengths and emission lifetimes. The extent of the interactions in the excited state (dimers, trimers, tetramers) is hard to predict because it depends on the amplitude of the interactions
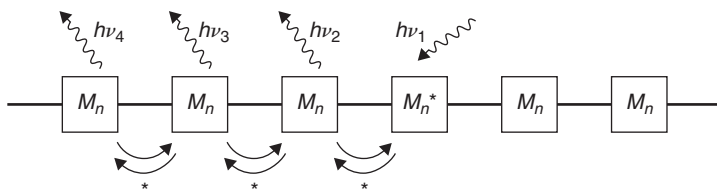
FIGURE 9. The excitation process.

and the relaxation rates. Hence the lifetime decay curve will have a poly-exponential nature.

VI. GROUND AND EXCITED STATE MOLECULAR INTERACTIONS

Ground state intermolecular interactions are present in some systems and require measurements of the binding constants. These interactions are manifested by the spectral changes experienced in the absorption spectra. Therefore, these changes can be monitored as a function of the concentration of the substrates leading to the extraction of the binding constants. On the other hand, intermolecular and intramolecular excited state interactions refer to the energy and electron transfer operating in the excited states of different dyad or polyad systems. These can also be excimers, dimers, or oligomers that are formed only in the excited states. Studies of photo-induced energy and electron transfers involve the measurement of their corresponding rates. The theory and methods used to characterize the different types of interactions are described next. Binding constant considerations are described elsewhere.[13]

A. Energy and Electron Transfer (Excited State Interactions and Reactions)

The possible deactivation pathways of the excited state are summarized in Figure 10. We discuss here the fluorescence and phosphorescence relaxation pathways and the thermal deactivation processes.

A transfer of the excitation energy from the donor to the acceptor will occur when an energy acceptor molecule is placed at the proximity of an excited energy donor molecule. After energy transfer, the donor relaxes to its ground state and the acceptor is promoted to one of its excited states. A photo-induced electron transfer can be initiated after photoexcitation when an excited single electron in the LUMO of the electron donor is transferred to a vacant molecular orbital (LUMO) of the acceptor.

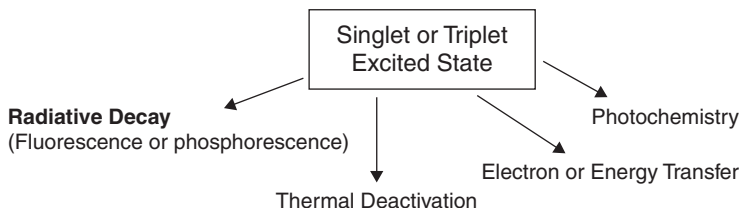The mechanisms for the energy and electron transfers are outlined below.

FIGURE 10. Different pathways for the deactivation of the excited state.

B. Energy Transfer

In presence of a molecule of a lower energy excited state (acceptor), the excited donor ($D*$) can be deactivated by a process known as energy transfer which can be represented by the following sequence of equations.

$$D + h\nu \rightarrow D* \tag{28}$$

$$D* + A \rightarrow D + A* \tag{29}$$

For energy transfer to occur, the energy level of the excited state of $D*$ has to be higher than that for $A*$ and the time scale of the energy transfer process must be faster than the lifetime of $D*$. Two possible types of energy transfers are known—namely, radiative and nonradiative (radiationless) energy transfer.

Radiative transfer occurs when the extra energy of $D*$ is emitted in form of luminescence and this radiation is absorbed by the acceptor (A).

$$D* \rightarrow h\nu + D \tag{30}$$

$$h\nu + A \rightarrow A* \tag{31}$$

For this to be effective, the wavelengths where the $D*$ emits need to overlap with those where A absorbs. This type of interaction operates even when the distance between the donor and acceptor is large (100 Å). However this radiative process is inefficient because luminescence is a three-dimensional process in which only a small fraction of the emitted light can be captured by the acceptor.

The second type, radiationless energy transfer, is more efficient. There are two different mechanisms used to describe this type of energy transfer: the Förster and Dexter mechanisms.

i. Förster Mechanism

The Förster mechanism is also known as the coulombic mechanism or dipole-induced dipole interaction. It was first observed by Förster.[14,15] Here the emission band of one molecule (donor) overlaps with the absorption band of another molecule (acceptor). In this case, a rapid energy transfer may occur without a photon emission. This mechanism involves the migration of energy by the resonant coupling of electrical dipoles from an excited molecule (donor) to an acceptor molecule. Based on the nature of interactions present between the donor and the acceptor, this process can occur over a long distances (30–100 Å). The mechanism of the energy transfer by this mechanism is illustrated in Figure 11.

In Figure 11, an electron of the excited donor placed in the LUMO relaxes to the HOMO, and the released energy is transferred to the acceptor via coulombic interactions. As a result, an electron initially in the HOMO of the acceptor is promoted to the LUMO. This mechanism operates only in singlet states of the donor and the acceptor. This can be explained on the basis of the nature of the interactions (dipole-induced dipole) because only multiplicity-conserving transitions possess large dipole moments. This can be understood considering the nature of the excited state in both the singlet and the triplet states. The triplet state has a diradical structure, so it is less polar, making it difficult to interact over long distances (i.e., Förster mechanism).

The rate of energy transfer (k_{ET}) according to this mechanism can be evaluated by the equation 32:[1]

$$k_{ET} = k_D R_F^6 \left(\frac{1}{R} \right)^6 \tag{32}$$

where k_D is the emission rate constant for the donor, R is the inter-chromophore separation, and R_F is the Förster radius, which can be defined as the distance between the donor and the acceptor at which 50% of the excited state decays by energy transfer—that is, the distance at which the energy transfer has the same rate constant as the excited state decay by the radiative and nonradiative channels ($k_{ET} = k_r + k_{nr}$). R_F is calculated by the overlap of the emission spectrum of the donor excited state (D^*) and the absorption spectrum of the acceptor (A).[1]
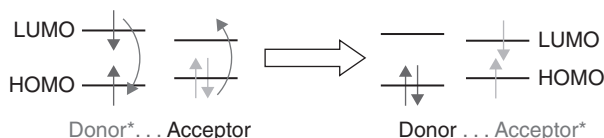

FIGURE 11. Mechanism of energy transfer action according to Förster.

ii. Dexter Mechanism

The Dexter mechanism is a nonradiative energy transfer process that involves a double electron exchange between the donor and the acceptor (Fig. 12).[16] Although the double electron exchange is involved in this mechanism, no charge separated-state is formed.

The Dexter mechanism can be thought of as electron tunneling, by which one electron from the donor's LUMO moves to the acceptor's LUMO at the same time as an electron from the acceptor's HOMO moves to the donor's HOMO. In this mechanism, both singlet-singlet and triplet-triplet energy transfers are possible. This contrasts with the Förster mechanism, which operates in only singlet states.

For this double electron exchange process to operate, there should be a molecular orbital overlap between the excited donor and the acceptor molecular orbital. For a bimolecular process, intermolecular collisions are required as well. This mechanism involves short-range interactions ($\sim 6-20$ Å and shorter). Because it relies on tunneling, it is attenuated exponentially with the intermolecular distance between the donor and the acceptor.[17] The rate constant can be expressed by the following equation.

$$k_{ET} = \frac{2\pi}{h} V_0^2 J_D \qquad \exp\left(-\frac{2R_{DA}}{L}\right) \qquad (33)$$

where R_{DA} is distance between the donor and the acceptor, J_D is the integral spectral overlap between the donor and the acceptor, L is the effective Bohr radius of the orbitals between which the electron is transferred, h is Plank's constant, and V_0 is the electronic coupling matrix element between the donor and acceptor at the contact distance.

Comparing the two energy transfer mechanisms, the Förster mechanism involves only dipole−dipole interactions, and the Dexter mechanism operates through electron tunneling. Another difference is their range of interactions. The Förster mechanism involves longer range interactions (up to $\sim 30-100$ Å), but the Dexter mechanism focuses on shorter range interactions (~ 6 up to 20 Å) because orbital overlap is necessary. Furthermore, the Förster mechanism is used to describe interactions between singlet states, but the Dexter mechanism can be used for both singlet-singlet and triplet-triplet interactions. Hence for the singlet-
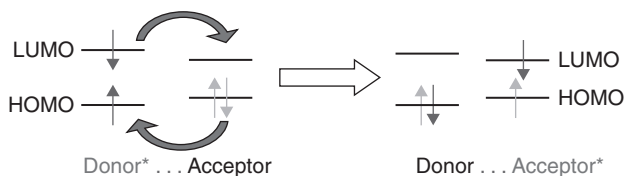

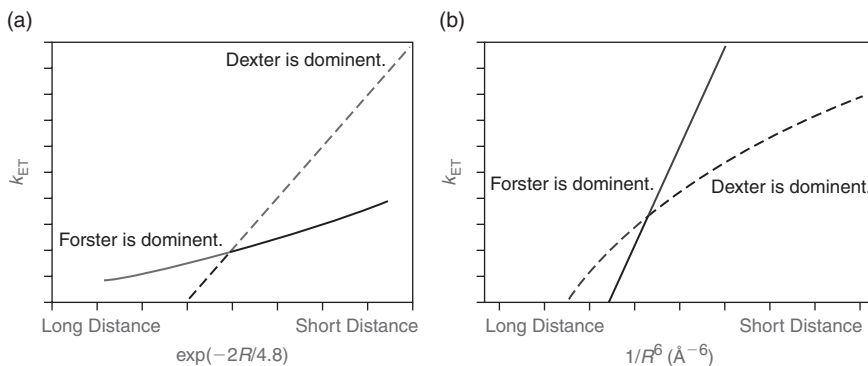**FIGURE 12.** Mechanism of energy transfer action according to the Dexter mechanism.

FIGURE 13. Qualitative theoretical plots for (a) and (b) k_{ET} versus $1/R^6$ (Förster). k_{ET} versus $\exp(-2R/4.8)$ (Dexter) (Modified from Ref. 18.)

singlet energy transfer, both mechanisms are possible. Simulated graphs using reasonable values for the parameters for the two mechanisms have been constructed for the purpose of distinguishing between the zones where Förster and Dexter mechanisms are dominant.[18] The experimental values of the energy transfer rates in cofacial bisporphyrin systems were found to agree with the theoretically constructed graphs (Fig. 13).[18]

In these graphs a Bohr radius value (L) of 4.8 Å (the value for porphyrin) is used in the Dexter equation 33.[18] Also, the solid lines correspond to hypothetical situations in which only the Förster mechanism operates; the dotted lines are hypothetical situations for when the Dexter mechanism is the only process.[18] The curved lines are simulated lines obtained with equation 32 (Förster) or 33 (Dexter) but transposed onto the other graph (i.e., Förster equation plotted against Dexter formulation and vice versa).

These plots clearly suggest the presence of a crossing point between the two mechanisms. There is a zone in which one mechanism is dominant and vice versa. All in all, the relaxation of an excited molecule via energy transfer processes will use all the pathways available to it so the total rate for energy transfer can be better described as k_{ET} (total) = k_{ET} (Förster)+k_{ET} (Dexter). According to Figure 13, the distance at which there is a change in dominant mechanism is ~ 5 Å.

C. Electron Transfer

Photo-induced electron transfer (PET) involves an electron transfer within an electron donor-acceptor pair. The situation is represented in Figure 14.

Photo-induced electron transfer represents one of the most basic photochemical reactions and at the same time it is the most attractive way to convert light energy or to store it for further applications. In Figure 14, one can see a

process taking place between a donor and acceptor after excitation, resulting in the formation of a charge separated state, which relaxes to the ground state via an electron-hole recombination (back electron transfer).

A theory used to study and interpret the photo-induced electron transfer in solution was described by Marcus.[19−25] In this theory, the electron transfer reaction can be treated by transition state theory where the reactant state is the excited donor and acceptor and the product state is the charge-separated state of the donor and acceptor (D^+-A^-), shown in Figure 15.

According to the Franck-Condon principle, the photoexcitation triggers a vertical transition to the excited state, which is followed by a rapid nuclear equilibration. Without donor excitation, the electron transfer process would be highly endothermic. However, after exciting the donor, electron transfer occurs at the crossing of the equilibrated excited state surface and the product state.

The change in Gibbs free energy associated with the electron transfer event is given by the following relation.[19]

$$\Delta G^{\#} = \frac{(\lambda + \Delta G^0)^2}{4\lambda} \tag{34}$$

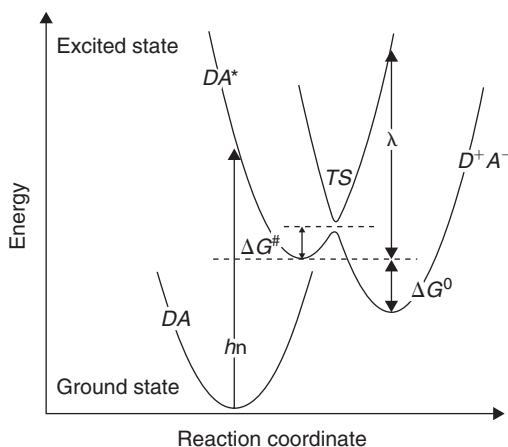**FIGURE 14.** Photo-induced electron transfer process.

FIGURE 15. Potential energy surfaces for the ground state (DA), the excited state (DA^*, reactant state), and the charge-separated state (D^+-A^-, product state), proposed by Marcus's theory. λ, total reorganization energy; TS, transition state. (Modified from Ref. 19.)

The total reorganization energy (λ), which is required to distort the reactant structure to the product structure without electron transfer, is composed of solvent (λ_S) and internal (λ_i) components ($\lambda = \lambda_i + \lambda_S$). The reaction free energy (ΔG^0), is the difference in free energy between the equilibrium configuration of the reactant (DA^*) and of the product states (D^+A^-). The internal reorganization energy represents the energy change that occurs in bond length and bond angle distortions during the electron transfer step and is usually represented by a sum of harmonic potential energies. In the classical Marcus theory, the electron transfer rate is given by equation 35.[22,22]

$$k_{ET} = \kappa_{ET}\nu_n \exp\left(\frac{-\Delta G^\#}{k_B T}\right) \tag{35}$$

where ν_n is the effective frequency of motion along the reaction coordinate and κ_{ET} is the electronic transmission factor.

The transmission factor is related to the transition probability (P_0) at the intersection of two potential energy surfaces, as given by the Landau-Zener theory.[24]

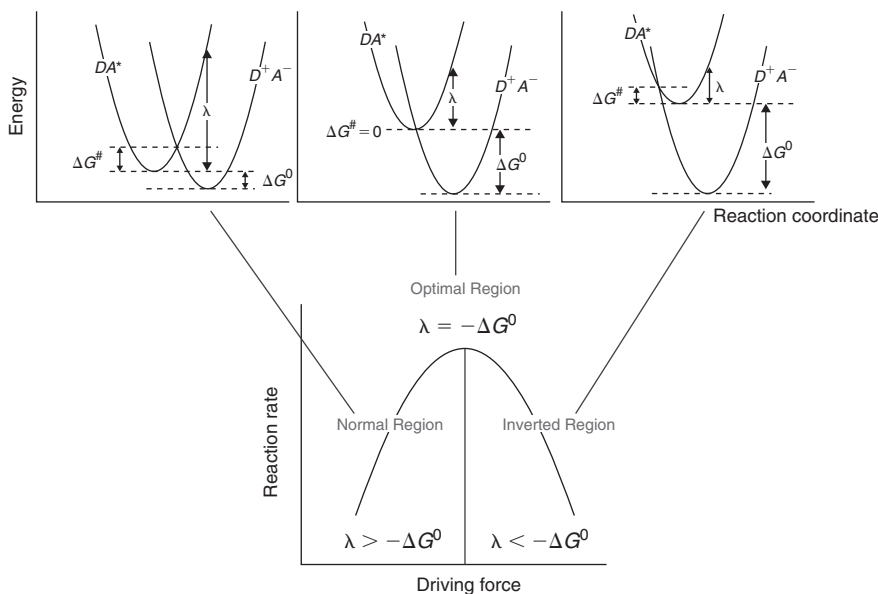$$\kappa_{ET} = \frac{2P_0}{1 + P_0} \tag{36}$$

FIGURE 16. The free energy regimes for electron transfer (top) and the corresponding reaction rate dependence on the free energy (bottom; driving force is ΔG^0-λ). (Modified from Ref. 19.)

A graph showing the change of the driving force for the electron transfer rate, calculated from Marcus theory, versus the rate constant is given in Figure 16 (bottom).

Using equation 35 to estimate the electron transfer rate, we can assign the Marcus normal region as that where the free reaction energy (ΔG^0) is decreased, leading to an increase of the electron transfer rate (k_{ET}). The second region that can be identified in Figure 16 is the optimal or activation-less region, where the driving force for electron transfer equals the reorganization energy—that is, $-\Delta G^0 = \lambda$. If ΔG^0 becomes even more negative, the activation barrier $\Delta G^{\#}$ reappears, resulting in a decrease in the values of k_{ET}. This last situation is observed over the region known as the inverted Marcus region and was first experimentally demonstrated by Closs and Miller.[25] The potential energy illustrating the different Marcus regimes can be seen in Figure 16 (top).

VII. NONLINEAR OPTICAL BEHAVIOR

Nonlinear optics (NLO) involves the interaction of light with materials resulting in a change in the frequency, phase, or other characteristics of the light. There are a variety of frequency-mixing processes. Second-order NLO behavior includes second harmonic generation of light that involves the frequency doubling of the incident light. Frequency mixing where the frequency of two light beams are either added or subtracted. Electrooptic effects can occur where both frequency and amplitude changes and where rotation of polarization occurs. NOL behavior has been found in inorganic and organic compounds and in polymers. The structural requirement is the absence of an inversion center requiring the presence of asymmetric centers and/or poling. Poling is the application of a high voltage field to a material that orients some or all of the molecule dipoles generally in the direction of the field. The most effective poling in polymers is found when they are poled above the T_g (which allows a better movement of chain segments) and then cooled to lock in the poled structure. Similar results are found for polymers that contain side chains that are easily poled. Again, cooling helps lock in the poled structure. At times, cross-linking is also employed to help lock in the poled structure.

Third-order NLO behavior generally involves three photons, resulting in effects similar to those obtained for second-order NLO behavior. Third-order NLO behavior does not require the presence of asymmetric structures.

Polymers that have been already been found to offer NLO behavior include polydiacetylenes and a number of polymers with liquid crystal side chains. Polymers are also employed as carriers of materials that themselves are NLO materials. Applications include communication devices, routing components, and optical switches.

VIII. PHOTOCONDUCTIVE AND PHOTONIC POLYMERS

Some polymeric materials become electrically conductive when illuminated with light. For instance, poly(*N*-vinylcarbazole) is an insulator in the dark, but when exposed to UV radiation it becomes conductive. The addition of electron acceptors and sensitizing dyes allows the photoconductive response to be extended into the visible and NIR regions. In general, such photoconductivity depends on the materials ability to create free-charge carriers, electron holes, through absorption of light, and to move these carriers when a current is applied.
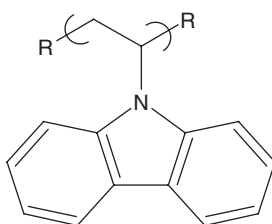

Poly(*N*-vinylcarbazole).

Related to this are materials whose response to applied light varies according to the intensity of the applied light. This is nonlinear behavior. In general, polymers with whole-chain delocalization or large-area delocalization in which electrons are optically excited may exhibit such nonlinear optical behavior.

A photoresponsive sunglass whose color or tint varies with the intensity of the sunlight is an example of nonliner optical material. Some of the so-called smart windows are also composed of polymeric materials whose tint varies according to the incident light. Currently, information is stored using electronic means but optical storage is becoming common place with the use of CD-ROM and WORM devices. Such storage has the advantages of rapid retrieval and increased knowledge density (i.e., more information stored in a smaller space).

Since the discovery of doped polyacetylene, a range of polymeric semiconductor devices has been studied, including normal transistors, field-effect transistors (FETs) photodiodes, and light-emitting diodes (LEDs). Like conductive polymers, these materials obtain their properties from their electronic nature, specifically the presence of conjugated π-bonding systems.

In electrochemical light-emitting cells, the semiconductive polymer can be surrounded asymmetrically with a hole-injecting material on one side and a low work function electron injecting metal (such as magnesium, calcium, or aluminum) on the other side. The emission of light may occur when a charge carrier recombines in the polymer as electrons from one side and holes from the other meet.

Poly(*p*-phenylene vinylene) (PPV) was the first reported (1990) polymer to exhibit electroluminescence.[26] PPV is employed as a semiconductor layer. The layer was sandwiched between a hole-injecting electrode and electron-injecting metal on the other. PPV has an energy gap of about 2.5 eV and thus produces a yellow-green luminescence when the holes and electron recombine. Today, many other materials are available that give a variety of colors.
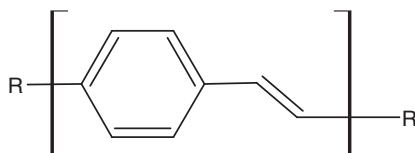
Poly(*p*-phenylene vinylene).

A number of poly(arylene vinylene) (PAV) derivatives have been prepared. Attachment of electron-donating substituents, such as two methoxy groups (**3**), act to stabilize the doped cationic form and thus lower the ionization potential.[26] These polymers exhibit both solvatochromism (color change as solvent is changed) and thermochromism (color is temperature dependent).
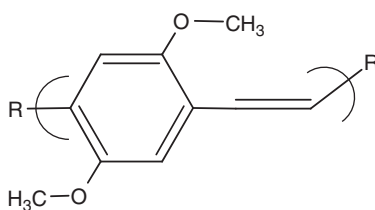
Poly(2,5-dimethoxy-*p*-phenylene vinylene).

The introduction of metals into polymers that can exhibit entire chain electron delocalization is at the basis of much that is presented in this volume. These metal-containing sites are referred to as *chromophores*, and the combination of metal chromophores exhibiting metal to ligand charge transfer (MLCT) excited states opens new possibilities for variation of electronic and optical properties needed for the continual advancement in electronics and electronic applications. Application areas include light-emitting polymeric diodes, solar energy conversion, and nonlinear optical materials and materials exhibiting photorefraction, electrochromism, and electrocatalysis.

One of the major reasons for interest in this area is the ease with which the new hybrid materials' properties can be varied by changing the metal, metal oxidation state, metal matrix, and polymer. Multiple metal sites are readily available. This allows the metal-containing system to have a high degree of tunability. This is due to the often strong electronic interaction between the metal

and the delocalized electron systems. The already noted variety of available metal sites is further leveraged by the increasingly capability of modern synthetic methodologies to achieve the desired structures. But the presence of metal atoms is at the heart of this.

IX. PHOTOSYNTHESIS

The recent environmental issues related to the greenhouse effect and atmospheric contamination heighten the importance of obtaining energy from clean sources, such as photosynthesis. Photosynthesis also acts as a model for the creation of synthetic light-harvesting systems that might mimic chlorophyll in its ability to convert sunlight into usable energy. The basis of natural photosynthesis was discovered by Melvin Calvin. Using carbon-14 as a tracer, Calvin and his team found the pathway that carbon follows in a plant during photosynthesis. They showed that sunlight supplies the energy through the chlorophyll site, allowing the synthesis of carbon-containing units, mainly saccharides or carbohydrates. Chlorophyll is a metal embedded in a protein polymer matrix and illustrates the importance of metals in the field of photochemistry and photophysics. A brief description of the activity of chlorophyll in creating energy from the sun follows.

The maximum solar power density reaching Earth is approximately 1350 W/m^2. When this energy enters the Earth's atmosphere, the magnitude reaching the surface drops approximately to 1000 W/m^2 owing to atmospheric absorption.[27,28] The amount that is used by plants in photosynthesis is about seven times the total energy used by all humans at any given time, thus it is a huge energy source.

Solar energy is clean and economical energy, but it must be converted into useful forms of energy. For example, solar energy can be used as a source of excitation to induce a variety of chemical reactions.

Natural examples for conversion of light energy are plants, algae, and photosynthetic bacteria that used light to synthesize organic sugar-type compounds through photosynthesis.

In photosynthesis, green plants and some bacteria harvest the light coming from the sun by means of their photosynthetic antenna systems. The light harvesting starts with light gathering by antenna systems, which consist of pigment molecules, including chlorophylls, carotenoids, and their derivatives. The absorbed photons are used to generate excitons, which travel via Förster energy transfers toward the reaction centers (RCs). This overall series of processes is represented in Figure 17.

In reaction centers, this energy drives an electron transfer reaction, which in turn initiates a series of slower chemical reactions. Energy is saved as redox energy,[29,30] inducing a charge separation in a chlorophyll dimer called the special
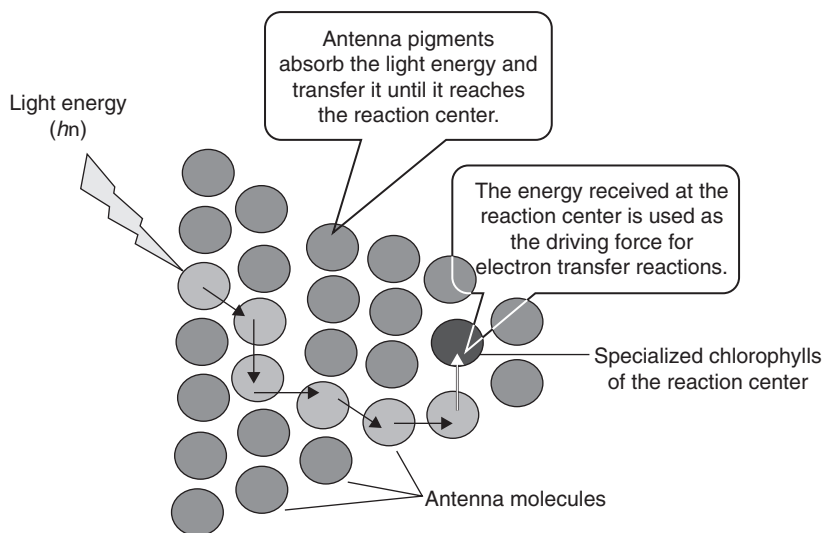
FIGURE 17. Light is absorbed by the antenna, and the energy is transferred to the reaction center, where charge separation takes place to generate chemical energy.

pair (chlorophyll)$_2$. Charge separation, which forms the basis for photosynthetic energy transfer, is achieved inside these reaction centers (eq. 37).

$$(\text{Chlorophyll})_2 + \text{Energy} \rightarrow (\text{Chlorophyll})_2^+ + e^- \tag{37}$$

Specialized reaction center proteins are the final destination for the transfered energy. Here, it is converted into chemical energy through electron-transfer reactions. These proteins consist of a mixture of polypeptides, chlorophylls (plus the special pair), and other redox-active cofactors. In the RCs, a series of downhill electron transfers occur, resulting in the formation of a charge separated state. Based on the nature of the electron acceptors, two types of reaction centers can be described. The first type (photosystem I) contains iron-sulfur clusters (Fe_4S_4) as their electron acceptors and relays, whereas the second type (photosystem II) features quinones as their electron acceptors. Both types of RCs are present in plants, algae, and cyanobacteria, whereas the purple photosynthetic bacteria contain only photosystem II and the green sulfur bacteria contain a photosystem I.[31,32] To gain a better understanding of these two types of RCs each will be further discussed.

A. Purple Photosynthetic Bacteria

In the mid-1980s, Deisenhofer reported his model for the structure of photosystem II for two species of purple photosynthetic bacteria (*Rhodopseudomonas viridis* and *Rhodobacter*) based on X-ray crystallography of

the light-harvesting device II (LH II).[33] Photosynthetic centers in purple bacteria are similar but not identical models for green plants. Because they are simpler and better understood, they will be described here. The photosynthetic membrane of purple photosynthetic bacteria is composed of many phospholipid-filled ring systems (LH II) and several larger dissymmetric rings (LH I) stacked almost like a honeycomb. Inside the LH I is a protein called the reaction center as illustrated in Figure 18.[34,35]

The LH II complex antenna is composed of two bacteriochlorophyll a (BCHl) molecules, which can be classified into two categories. The first one is a set of 18 molecules arranged in a slipped face-to-face arrangement and is located close to the membrane surface perpendicularly to these molecules. The second ring is composed of 9 BCHl in the middle of the bilayer. The first 18 BCHl have an absorption maximum at 850 nm and are collectively called B850, while the second (9 BCHl) have an absorption maximum at 800 nm and are called B800. These structures are contained within the walls of protein cylinders with radii of 1.8 and 3.4 nm. Once the LH II complex antenna absorbs light, a series of very complex nonradiative photophysical processes are triggered. First the excitation energy migrates via energy transfers involving the hopping of excitation energy within almost isoenergetic subunits of a single complex. This is followed by a fast energy transfer to a lower energy complex with minimal losses (Fig. 19). These ultrafast events occur in the singlet state (S_1) of the BCHl pigments and are believed to occur by a Förster mechanism.[34]

The energy collected by the LH II antenna is transferred to another antenna complex known as LH I, which surrounds the RC. The photosynthetic reaction centers of bacteria consist mainly of a protein that is embedded in and spans a lipid bilayer membrane. In the reaction center, a series of electron transfer reactions are driven by the captured solar energy. These electron transfer reactions convert the captured solar energy to chemical energy in the
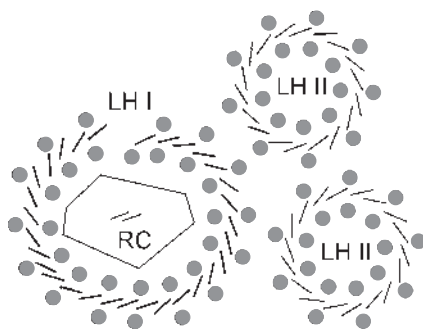

FIGURE 18. Two light-harvesting II (LH II) units next to one light-harvesting I (LH I) unit. *Gray circles*, polypeptides, *bars*, rings of interacting bacteriochlorophylls a (called B850). In the middle of LH I, there is the reaction center (RC), where the primary photo-induced electron transfer takes place from the special pair of bacteriochlorophylls b.[34]
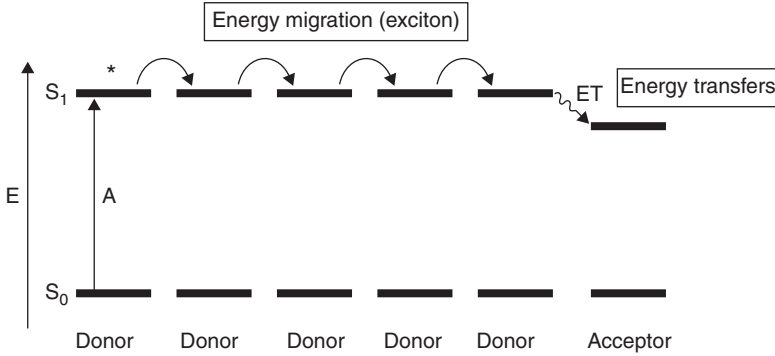
FIGURE 19. The exciton and energy transfer processes. (Modified from Ref. 8.)
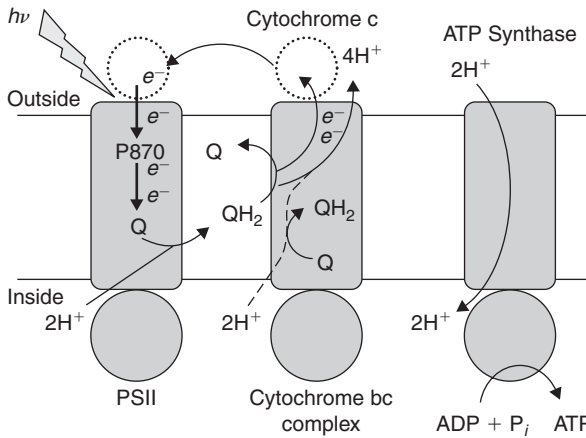

FIGURE 20. A cross-section of the photosynthetic membrane in the purple photo-synthetic bactemria. PS II, photosystem II; *P870*, special pair; *Q*, plastoquinone; *QH₂*, dihydroplastoquinone; *ADP*, adenosine diphosphate; *ATP*, adenosine triphosphate.

form of a charge separation process across the bilayer.[36−38] The mechanism of this process is illustrated in Figure 20.

A special BCHl (P870) pair is excited either by the absorption of a photon or by acquiring this excitation energy from an energy transfer from the peripheral antenna BCHl (not shown in the figure for simplicity), triggering a photoinduced electron transfer inside the RC.[36] Two photoinduced electrons are transferred to a plastoquinone located inside the photosynthesis membrane. This plastoquinone acts as an electron acceptor and is consequently reduced to a semiquinone and finally to a hydroquinone. This reduction involves the uptake of two protons from water on the internal cytoplasmic side of the membrane. This hydroquinone then diffuses to the next component of the apparatus, a proton pump called the cytochrome bc1 complex (Fig. 20).

The next step involves the oxidation of the hydroquinone back to a quinone and the energy released is used for the translocation of the protons across the membrane. This establishes a proton concentration and charge imbalance (proton motive force; pmf). Thus the oxidation process takes place via a series of redox reactions triggered by the oxidized special pair BCHl (P870), which at the end is reduced to its initial state. The oxidation process is ultimately driven, via various cytochrome redox relays, by the oxidized P870. Oxidized P870 becomes reduced to its initial state in this sequence. Finally, the enzyme ATP synthase allows protons to flow back down across the membrane driven by the thermodynamic gradient, leading to the release of ATP formed from adenosine diphosphate and inorganic phosphate (P_i). The ATP fills the majority of the energy needs of the bacterium.[37]

B. Green Sulfur Bacteria

The observation of a photosynthetic reaction center in green sulfur bacteria dates back to 1963.[39] Green sulfur bacteria RCs are of the type I or the Fe-S-type (photosystem I). Here the electron acceptor is not the quinine; instead, chlorophyll molecules (BChl 663, 8^1-OH-Chl a, or Chl a) serve as primary electron acceptors, and three Fe_4S_4 centers (ferredoxins) serve as secondary acceptors. A quinone molecule may or may not serve as an intermediate carrier between the primary electron acceptor (Chl) and the secondary acceptor (Fe-S centers).[40] The process sequence leading to the energy conversion in RC I is shown in Figure 21.
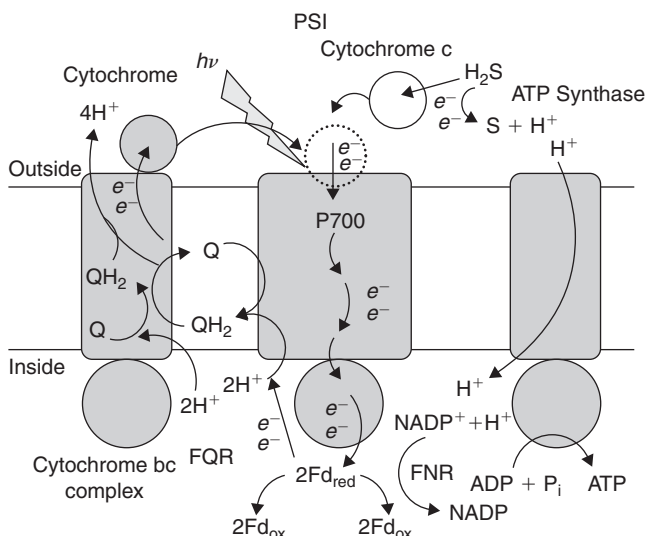

FIGURE 21. Photosystem I (PS I). P_{700}, special pair; Q, plastoquinone; QH_2, dihydroplastoquinone; $NADP$, nicotinamide adenine dinucleotide phosphate; FQR, ferredoxin-quinone reductase; FNR, ferredoxin-NADP reductase; Fd, ferredoxin; ADP, adenosine diphosphate; ATP, adenosine triphosphate.

A large number of chlorophyll antennas are used to harvest the solar energy, which in turn are used to excite the special pair P_{700}. The P_{700} donor will in turn transfer an electron to a primary acceptor (A_0, phyophytin) and in less than 100 ps to a secondary acceptor (A_1, a phylloquinone). The electron received by A_1 is in turn transferred to an iron-sulfur cluster and then to the terminal iron-sulfur acceptor.[41]

X. ORGANOMETALLIC POLYMERS AND SYNTHETIC PHOTOSYNTHESIS SYSTEMS

Organic and organometallic polymers exhibit potential applications in photonics. Organometallic polymers have received a lot of interest because they could combine the advantages of the high luminescence of the organic moiety with the high carrier density, mobility, steady chemical properties, and physical strength of inorganic materials. Research on such materials is expanding because of their potential use as electric components such as FETs, LEDs, and solar cells.

Much effort involving solar energy conversion is based on the natural chlorophyll system as a model. Here a metal atom is embedded within a polymer matrix that exhibits high electron mobility (delocalization). Ruthenium,[42−52] platinum,[53−59] and palladium[53−59] are the most employed metals. The use of materials containing the bis(2,2-bipyridine)ruthenium II moiety is common with ruthenium because this moiety absorbs energy in the UV region and emits it at energies approximating those needed to cleave water molecule bonds. The use of solar energy to create hydrogen that is harvested and later converted to useful energy has been a major objective.

Here we focus on a more direct conversion of solar energy into energy to charge batteries. For this purpose, metal-containing polymers can be classified into three types (types I, II, and III), as illustrated in Figure 22.[60,61] In type I, the metal centers are connected to the conjugated polymer backbone through saturated linkers, such as alkyl chains. Polymers of type I act as a conducting support. The electronic, optical, and chemical properties of the metal ions in
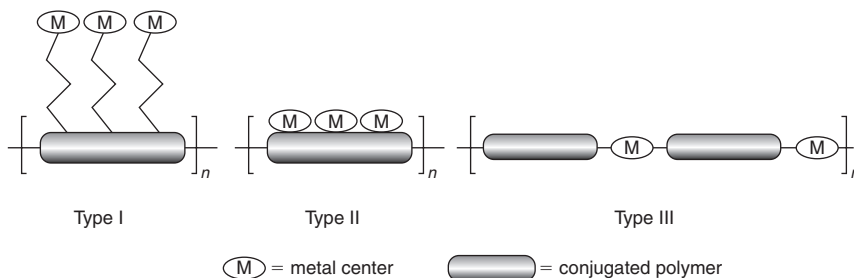

Type I   Type II   Type III

M = metal center   = conjugated polymer

FIGURE 22. Types of metal-containing polymers. (Modified from Ref. 61a.)

this type of polymer remain the same as they would be if they were alone (i.e., unattached to the polymer backbone). In the second type, the metal centers are electronically coupled to the conjugated polymer backbone. This affects both the polymer and the metal group properties. The metal centers for type III are located directly within the conjugated backbone. In this last type, there are strong interactions between the metal center and the organic bridge. For this arrangement, the electronic interactions between the organic bridge and the metal group are possible, and new properties can be obtained because of the combination of the characteristics of the organic polymers with the common properties of the transition metals.[60,61]

Heavy metal atoms in the polymer backbone increases the intersystem crossing rate of the organic lumophores due to enhanced spin-orbit coupling. This populates more of the triplet states facilitating the study of interactions on both singlet and triplet states.[61] The study of energy transfer in organic and organometallic polymers is important. In fact, various types of organic and organometallic systems (oligomers and polymers) have been specifically designed for intramolecular energy transfer studies. Molecular architecture was found to play an important role in the efficiency of the energy transfer. The bridge between the donor and the acceptor chromophores exerts an important effect on the rates as well as the mechanism through which the energy transfer occurs.[62,63] A through-bond mechanism operates very efficiently for the cases of rigid saturated hydrocarbon bridges, while through-space mechanism are efficient for flexible bridges.[64,65]

Harvey et al. studied the photophysical properties of macromolecules built on M-P and M-CN (isocyanide) bonds, including the metal in the backbone. (This topic is reviewed in Chapter 2. The presence of the metal atom associated with the porphyrin moiety is examined here.

Photosynthesis is a source of inspiration for scientists interested in non-natural systems that convert light into chemical potential or electrical energy. Molecular wires, optoelectronic gates, switches, and rectifiers are typical examples of molecular electronic devices envisioned for use in energy or electron transfer processes.[66−69] A basic device structure, stimulating the natural systems, needs a scaffold on which the energy or charge transfer can be induced. Such a scaffold is represented in Figure 23.

The approach for this system is the mimicry of the highly efficient photosynthesis process in biological systems, by which an antenna device collects the light energy before a series of exciton, energy, and electron transfers, which lead to the synthesis of the plant's fuel.[70−73]

Porphyrins are an interesting class of compounds used for the study of energy- and electron-transfer functions of the natural photosynthetic machinery. The interest in porphyrins is motivated in part by their photocatalytic activity and electronic properties.[74] Porphyrins are also structurally related to chlorophyll.

Cofacial bisporphyrin systems use rigid spacers to provide a unique placement of two chromophores (donor and acceptor) at a given distance,
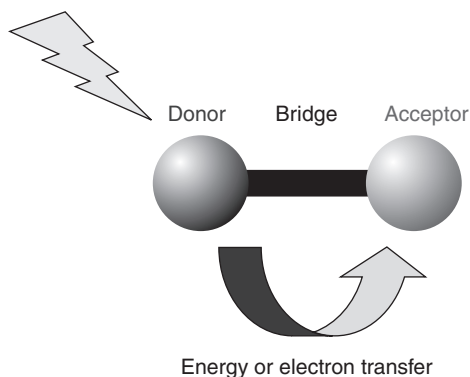
FIGURE 23. A scaffold for photo-induced intramolecular energy or electron transfer.
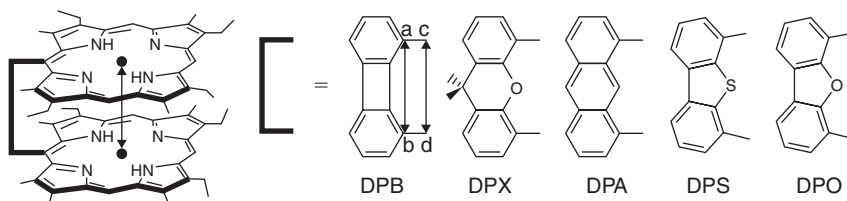

FIGURE 24. Examples of cofacial face-to-face porphyrin systems with different spacers. (Modified from Ref. 75.)

inducing a through-space energy transfer as the shortest pathway for inter-molecular interactions and communications.[75]

Recently, the effect of the donor-acceptor separation has been studied.[76] Both the fluorescence lifetime and quantum yield were found to decrease as the distance between the two porphyrins—C_{meso}-C_{meso} (cd) and CC_{meso}-CC_{meso} (ab)—decreases (Fig. 24). As the two rings get closer to each other, they interact more strongly, and hence nonradiative deactivation becomes more pronounced.[75,76]

The rate dependence for the S_1 energy transfer (S_1 ET) for such systems exhibits a dependence of the energy transfer (k_{ET}) rate on the C_{meso}-C_{meso} distance. The rate increases as the distance decreases.[75] Face-to-face donor-acceptor separations are on the order of ~ 3.5 Å verses the corresponding various donor-acceptor separations in the living supramolecular structures (found in plants, algae, and cyanobacteria) (Fig. 24 and 25) which are found to have separation distances to ~ 20 Å. Despite this observation, the S_1 energy transfer data are strikingly slower (two orders of magnitude).[34] This leads to the question, What is missing?

Both through-space and through-bond energy transfer mechanisms are known, by which singlet-singlet energy transfer occurs through both
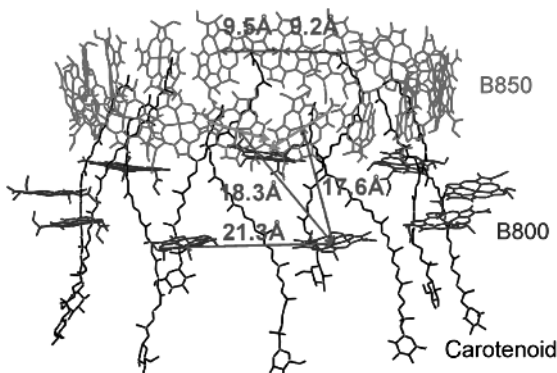
FIGURE 25. A LH II ring showing only the chlorophyll for the B850 network, the noninteracting B800 bacteriochlorophylls, and the rhodopin glucosides. Two of the B850 units are marked with *arrows*, representing the transition moments. (Modified from Ref. 34.)
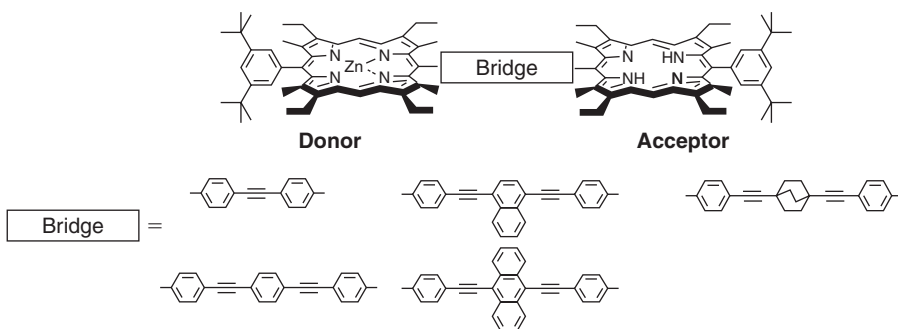

FIGURE 26. Some donor-bridge-acceptor systems by which energy transfer occurs through both Förster and Dexter mechanisms. (Modified from Ref. 78.)

Coulombic or dipole-dipole interaction (Förster) and double electron exchange (Dexter) mechanisms.

Different donor-bridge-acceptor based dyads based on metallated and free base porphyrins, by which singlet-singlet energy transfer occurs through both Förster and Dexter mechanisms are given in Figure 26.[77,78] The S_1 energy transfer in these systems occurs via a contribution from both coulombic and double electron exchange, which have almost the same magnitude and are not affected by the donor and acceptor distances. The electronic interactions depend on the donor-bridge energy gap and the bridge conformation (planar or nonplanar). Studies of the energy transfer rate as a function of the energy gap between the donor and the bridge have facilitated the separation of the two mechanisms. The rates observed for systems with the biggest energy gap were found to be almost equal to the Förster energy transfer rates.
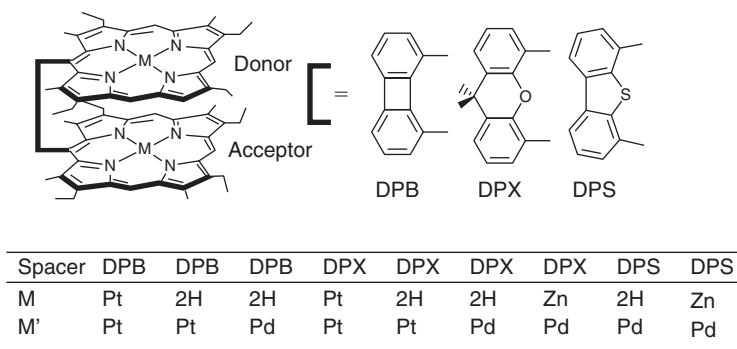
Spacer	DPB	DPB	DPB	DPX	DPX	DPX	DPX	DPS	DPS
M	Pt	2H	2H	Pt	2H	2H	Zn	2H	Zn
M'	Pt	Pt	Pd	Pt	Pt	Pd	Pd	Pd	Pd

FIGURE 27. Examples of cofacial bisporphyrin systems containing heavy atoms. (Modified from Ref. 75.)

Harvey's group studied energy transfers arising from the longer-lived triplet states as well as from the singlet states. These studies involved porphyrins containing a heavy metal (e.g., Pt and Pd), as shown in Figure 27.[79] Spin orbit coupling of the heavy atom increased the intersystem crossing rates, thus increasing the population of the triplet excited state. Triplet energy transfers can be analyzed only according to the Dexter mechanism because the Förster mechanism does not operate in the triplet excited states due to their diradical nature and the multiplicity change during the process. Energy transfer for the Dexter mechanism occurs via a double electron exchange—HOMO (acceptor)→HOMO(donor) and LUMO(donor)→LUMO (acceptor)—between triplet states of the donor and acceptor. In these systems (Fig. 27), the Pd- and Pt-metallated chromophores act as triplet donors, whereas the free base and Zn-containing complexes are the energy acceptors.

Analyses of energy transfer rates revealed that no sensitive transfer was detected for systems in which the spacer was DPS. In contrast, for dyads with the DPB and DPX spacers containing dyads, energy transfer occurred. This result was explained on the basis that singlet states energy transfer occurs via both Förster and Dexter mechanisms in the DPB- and DPX-containing dyads: C_{meso}-C_{meso} = 3.80 and 4.32 Å, respectively. The singlet energy transfer mechanism proceeded predominantly via a Dexter mechanism. Conversely, singlet energy transfer in the DPS-containing dyad, C_{meso}-C_{meso} = 6.33 Å, operated predominantly according to the Förster mechanism. This latter mechanism is inactive in the triplet states.[77] Thus, at such long distances, orbital overlap is poor and energy transfer is either weak or nil. This concept is of importance for designing molecular switches based on the distance separating the donor from the acceptor.

Through-bond energy transfer was also observed for porphyrin systems (regardless whether it occurs via a Förster or a Dexter mechanism). Through-bond energy transfer was reported for the rhodium meso-tetraphenylporphyrin-tin (2,3,7,13,17,18-hexamethyl-8,12-diethylcorrole), which exhibits a Rh-Sn bond
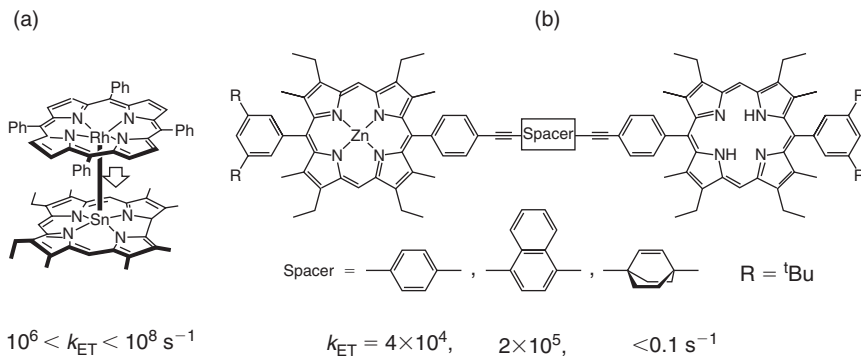
$10^6 < k_{ET} < 10^8 \text{ s}^{-1}$ $k_{ET} = 4 \times 10^4,$ $2 \times 10^5,$ $< 0.1 \text{ s}^{-1}$

FIGURE 28. Porphyrin systems with through-bond energy transfer.

length of 2.5069 Å and a 3.4 Å separation between the average macrocycle planes, Figure 28.[75]

A photophysical study of these porphyrin systems showed the presence of significant intramolecular triplet energy transfer with an estimated k_{ET} ranging between 10^6 and 10^8 s^{-1}. Rates for the through-bond process were found to be three to five orders of magnitude larger than the through-space energy transfer. Other examples for through-bond energy transfer are shown in Figure 28.[80,81] The intramolecular energy transfer rates within these systems were found to be slower than those estimated for cofacial systems by two or three orders of magnitude.[34] These results can be helpful in predicting the rates for energy transfer (k_{ET}) for unknown systems.

A similar observation was made by Albinson, using Zn(II)porphyrin as the donor and free base porphyrin as the acceptor. The solvent viscosity and temperature were investigated as factors affecting the donor-acceptor interactions (Fig. 29).[32] In this example, and in agreement with Figure 28,[75] the rate increased with an increase of conjugation. Conversely, energy transfer is completely turned off when the conjugation is broken by the presence of the saturated system. This indicates that the through-bond energy transfer process occurs from the higher energy triplet state of Zn(II)porphyrin to the lower lying triplet state of the free base porphyrin.

The triplet energy transfer rates were measured over temperatures from 295 K to 280 K. The free energies of activation were found to be in the range of 1.0–1.7 kcal/mol (about 4–8 kJ/mol) in low-viscosity solvents, whereas in high-viscosity solvents, the temperature dependence is less pronounced. The triplet energy transfer was dependent on the solvent viscosity. Dramatically slower rates are observed in high-viscosity solvents due to smaller electronic coupling. The triplet-excited donor porphyrin was suggested to adopt conformation in less viscous solutions, which have a much larger electronic coupling than is possible in highly-viscous media. The porphyrins considered in the study are prone to conformational change in the triplet-manifold. This was
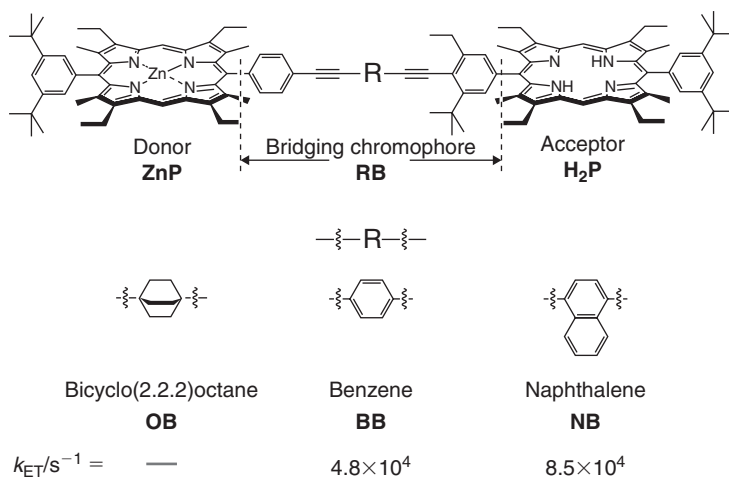
FIGURE 29. Porphyrin systems with through-bond energy transfer. (Modified from Ref. 82.)

explained on conformational grounds. In a donor-spacer-acceptor system (Fig. 29), with the ground state exhibiting a dihedral angle near 90°, the electronic coupling is changed in the triplet state to a situation in which the phenyl group should rotate toward the plane of the porphyrin macrocycle, leading to a considerable increase in the electronic coupling. This conformational freedom is lost when the solvent rigidifies, leading to a decrease in the coupling between the donor and the bridge. In solvents of low viscosity, another observation was made. Indeed, the change in temperature led to a triplet state distortion, inducing slower rates for triplet energy transfers.

All in all, the nature of the donor-acceptor linker is undoubtedly a controlling factor for the energy transfer, especially in the case of the triplet state interactions in which the mechanism of the interaction proceeds according to the Dexter mechanism (i.e., double electron exchange). This analysis illustrates the importance of studying different donor-acceptor spacers and their geometries during photo-induced energy transfer.

XI. SUMMARY

Interest in the electronic properties of π-conjugated oligomers and polymers and polymers containing metal atoms continues to increase greatly. The metal site can offer chromophores that exhibit metal to ligand charge transfer (MLCT) excited states in the π-conjugated polymers systems. This allows a variety of electronic and optical properties that are finding application in numerous areas, including solar energy conversion devices, nonlinear optical

materials (NLOs), and polymer light-emitting diodes (PLEDs), with applications in physical and chemical sensing, electrochromism, and a wide scope of electrocatalysis. The presence of the metal allows the synthesis of a wide variety of materials, with a variety of optical, electronic, chemical, and physical characteristics. The particular properties are changed and tuned by varying the metal, metal oxidation state, and metal environment. This volume describes some of these materials and applications for metal-containing sites embedded within polymer matrices and it suggests others.

XII. REFERENCES ADDITIONAL READINGS

N. S. Allen, *Photochemistry,* **36,** *232* (2007).

V. Balzani, S. Campagna, *Photochemistry and Photophysics of Coordination Compounds,* Springer Verlag, New York, 2007.

C. Carraher, *Polymer Chemistry,* 7th ed., Taylor & Francis, Boca Raton, FL, 2008.

R. Dessauer, *Photochemistry,* Elsevier, New York, 2006.

D. Neckers, *Advances in Photochemistry,* Wiley, Hoboken, NJ, 2007.

D. Phillips, *Polymer Photophysics,* 2nd ed., Springer, New York, 2007.

V. Ramamurthy, *Semiconductor Photochemistry and Photophysics,* CRC Press, Boca Raton, FL, 2003.

N. Turro, V. Ramamurthy, J. Scaiano, *Principles of Molecular Photochemistry,* University Science Books, New York, 2009.

XIII. REFERENCES

1. B. Valeur, *Molecular Fluorescence: Principles and Applications,* Wiley-VCH, Weinheim, Germany, 2002.

2. J. Michl, V. Bonacic-Koutechy, *Electronic Aspects of Organic Photochemistry,* Wiley Interscience, New York, 1990.

3. A. Khan, S. Muller, S. Hecht, *Chem. Commun., 584 (*2005).

4. J. N. Demas, G. A. Crosby, *J. Phys. Chem.,* **75,** *991* (1971).

5. D. F. Eaton, *Pure Appl. Chem.,* **60,** *1107* (1988).

6. C. Carraher, *Polymer Chemistry,* 7th ed., Taylor & Francis, New York, 2008.

7. E. U. Condon, G. H. Shortley, *The Theory of Atomic Spectra,* Cambridge University Press, Cambridge, UK, 1935.

8. R. Engleman, J. Jortner, *Mol. Phys.,* **18,** *145* (1970).

9. J. R. Lakowicz, *Topics in Fluorescence Spectroscopy,* vol. 1, *Techniques,* Kluwer Academic/Plenum Publishers, New York, 1999.

10. N. J. Turro, *Molecular Photochemistry,* Benjamin, New York, 1967.

11. J. R. Lakowicz, *Principles of Fluorescence Spectroscopy,* Springer, New York, 2006.

12. Nobel Lecture, 1967. http://nobelprize.org/nobel_prizes/chemistry/laureates/1967/porter-lecture.pdf.

13. K. A. Conors, *Binding Constants,* Wiley, New York, 1987.

14. T. H. Förster, *Ann. Phys., 2, 55* (1948).

15. T. H. Förster, *Discuss. Faraday Soc., 27, 7* (1959).

16. D. L. Dexter, *J. Chem. Phys., 21, 836* (1953).

17. A. Mistra, P. Kumar, M. Kalalasanan, S. Chandra, *Semicond. Sci. Technol., 21, R35* (2006).

18. S. Faure, C. Stern, R. Guilard, P. D. Harvey, *J. Am. Chem. Soc., 126, 1253* (2004).

19. R. A. Marcus, *Pure Appl. Chem., 69, 13* (1997).

20. R. A. Marcus, *Annu. Rev. Phys. Chem., 15, 155* (1964).

21. R. A. Marcus, *Angew. Chem., 105, 1161* (1993).

22. R. A. Marcus, *J. Chem. Phys., 24, 966* (1956).

23. R. A. Marcus, *J. Chem. Phys., 43, 679* (1965).

24. L. D. Landau, *Phys. Z. SSR., 2, 46* (1932).

25. J. R. Miller, J. Beitz, R. Huddleston, *J. Am. Chem. Soc., 106, 5057* (1984).

26. C. Carraher, *Introduction to Polymer Chemistry,* Taylor & Francis, New York, 2007.

27. N. J. Ekins-Daukes, M. Guenette, *Boomerang Trans., 1, 10* (2006).

28. (a) G. P. Smestad, *Optoelectronics of Solar Cells,* SPIE Press Washington, DC, 2002. (b) J. Rostalski, D. Meissner, *Sol. En. Mat. Sol. Cell., 61, 87* (200).

29. R. van Grondelle, J. Dekker, T. Gillbro, V. Sundsrom, *Biochem. Biophys. Acta, 1, 1187* (1994).

30. R. E. Blankenship, *Molecular Mechanisms of Photosynthesis,* Blackwell Science, Oxford, 2002.

31. R. E. Blankenship, *Photosynth. Res., 33, 91* (1992).

32. W. Hillier, G. Babcock, *Plant Physiol. J., 125, 33* (2001).

33. P. Heathcote, M. R. Jones, P. Fyfe, *Phil. Trans. R. Soc. Lond. B, 358, 231* (2003).

34. P. D. Harvey, C. Stern, C. Gros, R. Guilard, *J. Inorg. Biochem., 102, 395* (2008).

35. K. Iida, J. Inagaki, K. Shinohara, Y, Suemori, M. Ogawa, T. Dewa, M. Nango, *Langmuir, 21, 3069* (2005).

36. D. Gust, T. Moore, A. L. Moore, *Acc. Chem. Res., 34, 40* (2001).

37. X. Hu, T. Ritz, A. Damjanovic, F. Auternieth, K. Schulten, *Q. Rev. Biophys., 35, 1* (2002).

38. R. Horton, L. Moran, G. Schrimqeour, M. Perry, D. Rawn, *Principles of Biochemistry,* Pearson Prentice Hall, Upper Saddle River, NJ, 2006.

39. R. E. Blankenship, M. Madigan, C. E. Bauer, *Anoxygenic Photosynthetic Bacteria,* Kluwer Academic Publishers, Dordrecht, 2004.

40. J. M. Olson, *Photochem. Photobiol., 64, 1* (1996).

41. M. Guergova-Kuras, B. Boudreus, A. Joliot, P. Joliot, K. Redding, *PNAS, 98, 4437* (2001).

42. K. Metera, H. Steiman, *Polym. Mater. Sci. Eng., 95, 88* (2006).

43. A. Mozer, Y. Wada,, K. Jiang, N. Masaki, S. Yanagida, S. Mori, *Am. Inst. Physics., 89, 435* (2006).

44. K. Man, H. Wong, W. Chan, B. Aleksandra, E. Beach, S. Rozeveld, *Langmui, 22, 3368* (2006).

45. F. Krebs, M. Biancardo, *Sol. Energy Sol. Cells., 90, 142* (2006).

46. C. Carraher, *Macromolecules Containing Metal and Metal-like Elements,* vol. 7, Wiley, Hoboken, 2006, ch. 3.

47. C. Carraher, *Macromolecules Containing Metal and Metal-like Elements,* vol. 5. Wiley, Hoboken, 2005, ch. 13.

48. C. Carraher, A. Taylor-Murphy, *Polym. Mater. Sci. Eng.,* **76,** *409* (1997) and **86,** *291* (2002).

49. C. Carson, R. Gerhardt, R. Tannenbaum, *J. Phys. Chem.,* **111,** *14114* (2007).

50. C. Carraher, Q. Zhang, *Polym. Mater. Sci. Eng.,* **71,** *505* (1997) and **73,** *398* (1995).

51. C. Carraher, Q. Zhang, *Metal-Containing Polymeric Materials,* Plenum, NY, 1996.

52. F. Guo, Y. Kim, J. Reynolds, K. Schanze, *Chem. Commun.,* *1887* (2006).

53. W. Wong, X. Wang, Z. He, A. Djurisic, B. Aleksandra, C. Yip, K. Cheung, H. Wang, H. Wang, C. Mak, W. Chan, *Nature Mater.,* **6,** *521* (2007).

54. P. D. Harvey, Z. Michel, *Z. Inorg. Chem.,* **32,** *4721* (1993).

55. J. Berube, K. Gagnon, D. Fortin, A. Decken, P. D. Harvey, *Inorg. Chem.,* **45,** *2812* (2006).

56. S. Clement, L. Guyard, M. Knorr, S. Dilsky, C. Strohmann, M. Arroyo, *J. Organomet. Chem.,* **692,** *839* (2007).

57. D. Evard, S. Clement, D. Lucas, B. Ganquet, M. Knorr, C. Strohmann, A. Decken, Y. Mugnier, P. D. Harvey, *Inorg. Chem.,* **45,** *1305* (2006).

58. I. Feinstein, *Rev. Inorg. Chem.,* **13,** *1* (1993).

59. I. Feinstein-Jaffe, A. Efrati, *J. Mol. Cat.,* **35,** 255 (1986) and **40,** *1* (1987).

60. W.-Y. Wong, S. Poon, *J. Inorg. Polym.,* **18,** *155* (2008), and references therein.

61. (a) M. O. Wolf, *Adv. Mater.,* **13,** *545* (2001). (b) W.-Y. Wong, *JIOPM,* **15,** *197* (2005).

62. A. Sen, V. Krishna, *Chem. Phys. Lett.,* **294,** *499* (1998).

63. N. Mataga, H. Yao, T. Okada, Y. Kanada, Y. A. Harriman, *Chem. Phys.,* **131,** *473* (1989).

64. D. Holten, D. Bocian, J. Lindsey, *Acc. Chem. Res.,* **35,** *57* (2002).

65. (a) S. L. James, *Coord. Rev.,* **276,** *32* (2003). (b) T. Tanase, *Bull. Chem. Soc. Jpn.,* **75,** *1407* (2002).

66. (a) J. M. Tour, *Acc. Chem. Res.,* **33,** *791* (2000). (b) R. W. Wagner, J. S. Lindsey, *J. Am. Chem. Soc.,* **116,** *9759* (1994).

67. (a) R. W. Wagner, J. S. Lindsey, J. Seth, V. Palaniappan, D. J. Bocia, *J. Am. Chem. Soc.,* **118,** *3996* (1996). (b) A. P. Silva, I. Dioxon, H. Gunaratne, T. Gunnlaughsson, P. Maxwell, T. E. Rice, *J. Am. Chem. Soc.,* **121,** *1393* (1999).

68. A. S. Martin, J. R. Sambles, *Physics Rev. Lett.,* **70,** *218* (1993).

69. D.H. Waldeck, D. N. Beratan, *Science,* **261,** *576* (1993).

70. P. D. Harvey in K. M. Kadish, K. M. Smith, R. Guildard, eds., *The Porphyrin Handbook,* vol. 18, Academic Press, San Diego, CA, 2003, and references therein.

71. X. Peng, N. Aratani, A. Takagi, T. Masumoto, T. Kawal, I. Hwang, T. Ahn, D. Kim, A. Osuka, *J. Am. Chem. Soc.,* **126,** *4468* (2004).

72. R. Takahashi, Y. Kobuke, *J. Am. Chem. Soc.,* **125,** *2372* (2003).

73. D. Kim, A. Osuka, *Acc. Chem. Res.,* **37,** *735* (2004).

74. J. Foekema, A. Schenning, D. Vriezema, F. Benneker, K. Norgaard, J. Kroon, T. Bjornholm, M. Feiters, A. Rowan, R. Nolte, *J. Phys. Org. Chem.,* **14,** *501* (2001), and references therein.

75. P.D. Harvey, C. Stern, C. Gros, R. Guilard, *Coord. Chem. Rev.,* **251,** *401* (2007).

76. F. Bolze, C. P. Gros, M. Drouin, E. Espinosa, P. D. Harvey, R. Guilard, *J. Organomet. Chem.,* **643−644,** *89* (2002).

77. S. Faure, C. Stern, E. Espinosa, J. Douville, R. Guilard, P. D. Harvey, *Chem. Eur. J.,* **11,** *3469* (2005).

78. (a) A. Kyrchenko, B. Albinsson, *Chem. Phys. Lett.,* **366,** *291* (2002). (b) K. Pettersson, A. Kyrchenki, E. Ronnow, T. Ljungdahl, J. Martensson, B. Albinsson, *J. Phys. Chem. A.,* **110,** *310* (2006).

79. J. Poulin, C. Stern, R. Guilard, P. D. Harvey, *Photochem. Photobiol.,* **82,** *171* (2006).
80. K. Kilsa, J. Kajanus, J. Martensso, B. Albinsson, *J. Phys. Chem. B.,* **103,** *7329* (1999).
81. J. Andreasson, J. Kajanus, J. Martensson, B. Albinsson, *J. Am. Chem. Soc.,* **122,** *9844* (2000).
82. J. Andreasson, A. Kyrychenki, J. Martensson, B. Albinsson, *Photochem. Photobiol. Sci.,* **1,** *111* (2002).